LETTER

doi:10.1038/nature10880

Adaptive radiation of multituberculate mammals before the extinction of dinosaurs

Gregory P. Wilson[1], Alistair R. Evans[2], Ian J. Corfe[3], Peter D. Smits[1,2], Mikael Fortelius[3,4] & Jukka Jernvall[3]

The Cretaceous–Paleogene mass extinction approximately 66 million years ago is conventionally thought to have been a turning point in mammalian evolution[1,2]. Prior to that event and for the first two-thirds of their evolutionary history, mammals were mostly confined to roles as generalized, small-bodied, nocturnal insectivores[3], presumably under selection pressures from dinosaurs[4]. Release from these pressures, by extinction of non-avian dinosaurs at the Cretaceous–Paleogene boundary, triggered ecological diversification of mammals[1,2]. Although recent individual fossil discoveries have shown that some mammalian lineages diversified ecologically during the Mesozoic era[5], comprehensive ecological analyses of mammalian groups crossing the Cretaceous–Paleogene boundary are lacking. Such analyses are needed because diversification analyses of living taxa[6,7] allow only indirect inferences of past ecosystems. Here we show that in arguably the most evolutionarily successful clade of Mesozoic mammals, the Multituberculata, an adaptive radiation began at least 20 million years before the extinction of non-avian dinosaurs and continued across the Cretaceous–Paleogene boundary. Disparity in dental complexity, which relates to the range of diets, rose sharply in step with generic richness and disparity in body size. Moreover, maximum dental complexity and body size demonstrate an adaptive shift towards increased herbivory. This dietary expansion tracked the ecological rise of angiosperms[8] and suggests that the resources that were available to multituberculates were relatively unaffected by the Cretaceous–Paleogene mass extinction. Taken together, our results indicate that mammals were able to take advantage of new ecological opportunities in the Mesozoic and that at least some of these opportunities persisted through the Cretaceous–Paleogene mass extinction. Similar broad-scale ecomorphological inventories of other radiations may help to constrain the possible causes of mass extinctions[9,10].

Multituberculate mammals were a taxonomically rich[3,11] and numerically abundant[12] clade that had originated by the Middle Jurassic epoch (approximately 165 million years (Myr) ago) and went extinct in the late Eocene (approximately 35 Myr ago)[3,11]. They were nearly globally distributed[13] and had a distinctive dentition consisting of procumbent incisors, blade-like premolars, molars with longitudinal rows of cusps (Fig. 1) and a predominantly posteriorly directed (palinal) chewing motion[14,15].

Palaeontologists have agreed for a long time that the success of multituberculate mammals was at least partly related to their highly derived dentition. Despite this, there is little consensus on the interpretations of their feeding ecology, perhaps owing to the limitations of previous approaches. For example, toothwear analysis is time intensive

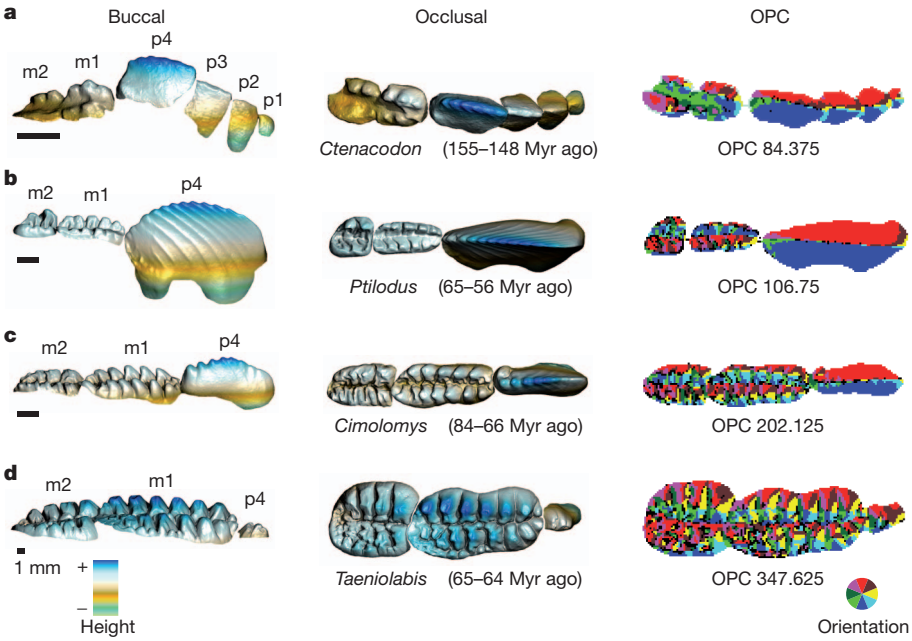

Figure 1 |
Dental and dietary diversity in multituberculate mammals. a–d, Three-dimensional buccal–occlusal and occlusal reconstructions of multituberculate lower-right cheek tooth rows for GIS analysis: Late Jurassic plagiaulacid *Ctenacodon serratus* (**a**), Paleocene ptilodontoid *Ptilodus kummae* (**b**), Late Cretaceous cimolomyid *Cimolomys gracilis* (**c**), Paleocene taeniolabidid *Taeniolabis taoensis* (**d**). Surface orientation map of each three-dimensional reconstruction (colour wheel indicates orientation) for OPC measurements (shown by the number of coloured patches). Clumps that are smaller than three grid points (black) are ignored. p, premolar; m, molar. Scale bars, 1 mm.

[1]Department of Biology, University of Washington, Seattle, Washington 98195-1800, USA. [2]School of Biological Sciences, Monash University, Victoria 3800, Australia. [3]Developmental Biology Program, Institute of Biotechnology, University of Helsinki, PO Box 56, FIN-00014, Helsinki, Finland. [4]Department of Geosciences and Geography, University of Helsinki, PO Box 64, FIN-00014, Helsinki, Finland.

and requires high-quality preservation[15], and multituberculates lack living descendants and this hampers comparative studies. Interpretations of multituberculate feeding ecology therefore vary widely; they have been proposed to be broad herbivores, frugivores, granivores, root- and bark-eaters, egg-eaters, insectivores, carnivores and omnivores[15–17].

To obtain a robust and comprehensive view of multituberculate ecomorphological diversity through time, we quantified dental complexity in 41 genera using geographic information systems (GIS) analyses[18] of three-dimensional crown surfaces of lower cheek teeth (Fig. 1; Supplementary Table 1). These analyses do not require cusp and facet homologies to be established, which can be a challenging task when comparing morphologically and phylogenetically divergent taxa. Orientation patch count (OPC), a measure of dental complexity, was calculated as the number of discrete surfaces on the cheek tooth row distinguished by differences in orientation (for example, north, southwest; Fig. 1). Extant rodents, carnivorans and bats demonstrate a robust correlation between OPC and feeding ecology; OPC increases across the dietary spectrum from carnivores to omnivores to herbivores, despite many differences in specific tooth components, body size and chewing mechanics among these taxa[18,19]. For a given clade, the standard deviation of OPC is an effective proxy for the dietary diversification and divergence in feeding function: higher standard deviation means greater dental disparity and a broader range of diets. OPC thus offers promise as a powerful tool for quantifying overall tooth shape and inferring diet in extinct taxa, such as multituberculates, that have highly derived dentitions with uncertain homology with living mammals and imprecise functional analogy.

Among the earliest multituberculates, the 'Plagiaulacida' are a paraphyletic assemblage of taxa with up to four simple blade-like premolars and two multi-cusped molars (Fig. 1a). OPC analyses of 'plagiaulacids' from the Late Jurassic through to the Early Cretaceous epoch (from 156–100 Myr ago) show low and tightly constrained dental complexity (Fig. 2a; OPC, 84–125). Their OPC values correspond to carnivory and the low end of animal-dominated omnivory among extant mammals (for example, eating both insects and fruits). Multituberculates in the early Late Cretaceous (100–84 Myr ago), which include mostly basal members of the suborder Cimolodonta, had a slightly higher mean OPC than did the 'plagiaulacids' but retained the low standard deviation of OPC (Fig. 2a), indicating low morphological disparity. A distinct break occurred 84–66 Myr ago, in the latest Cretaceous, when the mean OPC rose and peaked within the Campanian (mean OPC, 145) and maximum OPC and disparity sharply increased as well (Fig. 2a; OPC, 70–230). Of the 17 taxa for this interval, 5 have OPC values that are greater than 160 and 2 have OPC values that are greater than 200, corresponding to values for plant-dominated omnivory and herbivory among extant mammals, respectively (Fig. 2a).

Finally, in the early Paleocene (66–62 Myr ago) multituberculates maintained high OPC (mean OPC, 138) and disparity peaked (Fig. 2a; OPC, 70–348). The early Paleocene *Taeniolabis* from North America (Fig. 1d) had the highest OPC among multituberculates (OPC, 348), which exceeded OPC values of extant herbivorous rodents and carnivorans[18]. Of the 16 other early Paleocene taxa, 4 have OPC values greater than 160 and 1 has an OPC value greater than 200 (Fig. 2a). Mean OPC and disparity of OPC declined during the remainder of the Paleocene and in the early Eocene (62–49 Myr ago). *Ectypodus*, the only known genus from the middle to late Eocene (49–35 Myr ago), has a low OPC (109), corresponding to the high end of the range for extant mammalian carnivores. This sharp drop in dental ecomorphological

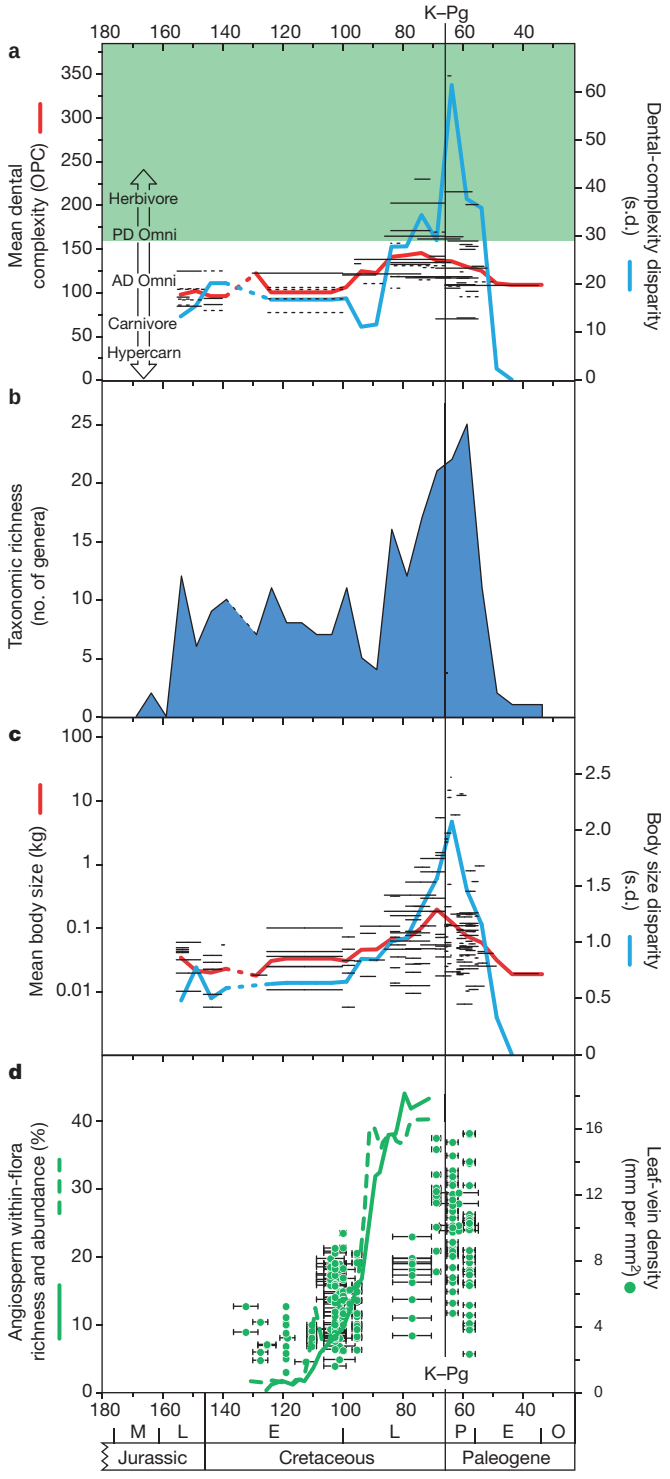

Figure 2 | Temporal patterns of multituberculate dental complexity, taxonomic richness, body size and angiosperm ecological diversification. **a**, Dental complexity (measured by OPC) for 41 multituberculate genera (solid black lines) and estimated for 24 additional genera (dashed black lines; see Supplementary Information) with mean dental complexity (OPC; red line) and disparity as standard deviations of OPC (blue line) in 5-Myr bins. Lengths of horizontal lines represent temporal ranges of taxa or uncertainties in ages of fossil localities. Labels for dietary classes are positioned at the lower end of their range based on OPC values in modern mammals[18]. Green shaded area represents plant-dominated omnivory (PD omni) and herbivory. **b**, Taxonomic richness is equal to the number of genera per 5-Myr bin (blue shaded area). **c**, Body-mass estimates for 156 multituberculate species (solid black lines) with geometric means (red line) and disparity (blue line) for each 5-Myr bin. **d**, Angiosperm within-flora richness (solid green line) and relative abundance (dashed green line) from ref. 24 (±7.5-Myr moving averages). Leaf hydraulic capacity of angiosperms as leaf-vein density (green circles) from ref. 25. The 136–131-Myr bin was excluded from all analyses (Supplementary Information). AD omni, animal-dominated omnivory; E, early; Hypercarn, hypercarnivory; M, middle; L, late; O, Oligocene; P, Paleocene.

disparity is intriguing in light of the hypothesis that some late Paleocene to early Eocene eutherian lineages (for example, rodents) competitively displaced multituberculates[12].

Variable sampling of fossils through time may influence our inferred patterns of multituberculate radiation. In particular, the relatively depauperate Jurassic and Early Cretaceous taxonomic richness of multituberculates may be partly due to the limited fossil record[3]. To test whether the changes in OPC through time might be sensitive to uneven sampling of fossils, we randomized the OPC value assignments for each genus. The results of 5,000 randomized mean OPC profiles through time indicate that even with additional fossil discoveries, the OPC patterns and ecological inferences that are presented here are likely to be robust (see Supplementary Fig. 8).

The overall trend of increasing multituberculate dental complexity was driven by increases in the number of cusps per molar and the relative size of molars in the cheek tooth row (Supplementary Fig. 1). This evolutionary pathway differs from that taken by ungulates, primates, rodents and lagomorphs, which responded to increased mechanical processing demands (that is, greater plant component) by evolving multi-cusped, molar-like premolars in addition to complex molars[20]. Among several other mammalian lineages with blade-like premolars (for example, carpolestid primates and potoroid marsupials), only sthenurine marsupials re-evolved multi-cusped premolars[21]. Developmental, functional or structural constraints that are associated with the evolution of a blade-like premolar may have inhibited later evolution of more cuspidate premolars.

Patterns of generic richness and conservative estimates of body size for multituberculates (see Methods Summary) mirror the pattern of initially low dental complexity for most of the Mesozoic followed by a marked increase just before the end of the Cretaceous (84–66 Myr ago; Fig. 2b, c). From the Late Jurassic to the early Late Cretaceous, multituberculate generic richness fluctuated between 4 and 16 genera, and body mass ranged between 9 g and 105 g. A marked shift occurred near the end of the Cretaceous, with generic richness increasing from 16 to 21 genera and average body mass increasing from 67 g to 194 g, in particular, *Bubodens magnus* reached an estimated 5.25 kg (for a comparison, the alpine marmot weighs 3–8 kg). Similarly, Cenozoic generic richness and body size patterns parallel changes in dental complexity (Fig. 2b, c). However, it should be noted that body size and dental complexity are not interchangeable as predictors of diet because small multituberculates can have high OPC values, and large multituberculates can have low OPC values (Supplementary Information), conforming to previous analyses of extant taxa[18]. Furthermore, variation in the amount of available fossil-bearing rock through the studied interval could contribute to the pattern of generic richness[22].

It is worth noting that increases in dental complexity (OPC of greater than 160) occurred in five multituberculate lineages: in the Asian Djadochtatheroidea, the North American Eucosmodontidae and Cimolomyidae (just before the end of the Cretaceous), the North American and Asian Taeniolabididae, and the North American Microcosmodontidae (in the early Paleocene). In the absence of a robust multituberculate phylogeny, it is unclear whether this represents a single evolutionary increase in tooth complexity, with multiple reversals to low complexity, or parallel increases in individual lineages or clades. This increase differs from the more commonly observed pattern, in which increased morphologic disparity precedes taxonomic diversification[23], as this increase occurred in step with an increase in multituberculate body size and taxonomic richness.

Overall, the pattern of increasing dental complexity in multituberculate mammals that pre-dates the Cretaceous–Paleogene mass extinction event contrasts with conventional ideas that mammalian evolution was suppressed during the Mesozoic era by selective pressures imposed by dinosaurs. Instead, multituberculates, the mammalian clade that co-existed for the longest time with non-avian dinosaurs, initiated an evolutionary radiation during the acme of dinosaur diversity, approximately 20 Myr before the Cretaceous–Paleogene boundary[22]. This is consistent with the highly specialized adaptations that are found among several new, exceptionally well-preserved Mesozoic mammal specimens[5] and with the timing of increased molecular divergence rates among extant mammalian lineages[6,7], but the multituberculates also show broad taxonomic and ecomorphologic diversification at the intraordinal level.

This adaptive response post-dated the taxonomic radiation of angiosperms but coincided broadly with increases in ecological diversity, abundance and leaf hydraulic capacities of angiosperms in the Late Cretaceous (in the Campanian and Maastrichtian)[8,24,25] (Fig. 2d), suggesting that there is a causal link. Many angiosperms during this time were herbaceous, and had a rapid life cycle and less-effective herbivore defences compared to other seed plants and would consequently have been an attractive, protein-rich food source for herbivores[26]. Some angiosperms had begun inhabiting a broader range of niches (trees, herbs and epiphytes) than most other plant groups and this may have enabled greater partitioning of the herbivore niche. Therefore, the multituberculate adaptive radiation, suggested by the increasing dental complexity, may have been triggered mainly by new niche space that was generated through the evolutionary and ecological radiations of angiosperms, but may have also been influenced by parallel radiations of associated non-angiosperm clades (for example, ferns[27]), insect pollinators, dispersers and herbivores[28]. A trophic link between angiosperms and some multituberculates is supported by our inferred dietary trend towards increased plant-dominated omnivory and herbivory among multituberculates just before the end of the Cretaceous and in the early Paleocene.

Our data also show that the dietary range of multituberculates did not decrease in response to the Cretaceous–Paleogene mass extinction event (Fig. 2a). Despite substantial taxonomic turnover of multituberculates at the Cretaceous–Paleogene boundary[29], they seem to have experienced little change in available food resources during one of the most severe extinction events in Earth's history. This apparent indifference of the multituberculate radiation to the Cretaceous–Paleogene event underscores the ecological selectivity of extinctions and suggests that broad-scale ecomorphological inventories of radiations may help to constrain the possible causes of extinction for other groups at the Cretaceous–Paleogene boundary[9,10].

METHODS SUMMARY

We scanned 48 dentitions from 41 genera of multituberculates. The three-dimensional scans of lower cheek tooth rows were analysed using GIS to quantify the number of discrete orientation patches using eight orientation directions. The mean of repeated measurements for eight rotations at multiples of 5.625° was used to reduce the effect of slight variations in the orientation of teeth. We compiled generic richness data from recent compendia and the primary literature. We estimated body mass from skull length, whenever available, and a tooth size to skull length regression formula. Detailed methods and calculations of dental complexity, generic richness and estimated body mass, data sets, measurements, calculations, randomization analyses and additional references are provided in the Supplementary Information.

Received 26 September 2011; accepted 20 January 2012.
Published online 14 March 2012.

1. Alroy, J. The fossil record of North American mammals: evidence for a Paleocene evolutionary radiation. *Syst. Biol.* **48,** 107–118 (1999).
2. Smith, F. A. *et al.* The evolution of maximum body size of terrestrial mammals. *Science* **330,** 1216–1219 (2010).
3. Kielan-Jaworowska, Z., Cifelli, R. L. & Luo, Z.-X. *Mammals from the Age of Dinosaurs: Origins, Evolution, and Structure* (Columbia Univ. Press, 2004).
4. Van Valen, L. M. & Sloan, R. E. Ecology and the extinction of the dinosaurs. *Evol. Theory* **2,** 37–64 (1977).
5. Luo, Z.-X. Transformation and diversification in early mammalian evolution. *Nature* **450,** 1011–1019 (2007).
6. Bininda-Emonds, O. R. P. *et al.* The delayed rise of present-day mammals. *Nature* **446,** 507–512 (2007).
7. Meredith, R. W. *et al.* Impacts of the Cretaceous terrestrial revolution and KPg extinction on mammal diversification. *Science* **334,** 521–524 (2011).
8. Wing, S. L. & Boucher, L. D. Ecological aspects of the Cretaceous flowering plant radiation. *Annu. Rev. Earth Planet. Sci.* **26,** 379–421 (1998).

9. Archibald, J. D. *et al.* Cretaceous extinctions: multiple causes. *Science* **328,** 973 (2010).
10. Schulte, P. *et al.* The Chicxulub asteroid impact and mass extinction at the Cretaceous-Paleogene boundary. *Science* **327,** 1214–1218 (2010).
11. Weil, A. & Krause, D. W. in *Evolution of Tertiary Mammals of North America* Vol. 2 (eds Janis, C. M., Gunnell, G.F. & Uhen, M. D.) 19–38 (Cambridge Univ. Press, 2008).
12. Krause, D. W. in *Vertebrates, Phylogeny, and Philosophy* (eds Flanagan, K.M. & Lillegraven, J.A.) 119–130 (Contributions to Geology, 1986).
13. Rich, T. H. *et al.* An Australian multituberculate and its palaeobiogeographic implications. *Acta Palaeontol. Pol.* **54,** 1–6 (2009).
14. Gingerich, P. D. in *Patterns of Evolution* (ed. Hallam, A.) 469–500 (Elsevier, 1977).
15. Krause, D. W. Jaw movement, dental function, and diet in the Paleocene multituberculate *Ptilodus*. *Paleobiology* **8,** 265–281 (1982).
16. Cope, E. D. The tertiary Marsupialia. *Am. Nat.* **18,** 686–697 (1884).
17. Simpson, G. G. The ''plagiaulacoid'' type of mammalian dentition. *J. Mamm.* **14,** 97–107 (1933).
18. Evans, A. R., Wilson, G. P., Fortelius, M. & Jernvall, J. High-level similarity of dentitions in carnivorans and rodents. *Nature* **445,** 78–81 (2007).
19. Santana, S. E., Strait, S. & Dumont, E. R. The better to eat you with: functional correlates of tooth structure in bats. *Funct. Ecol.* **25,** 839–847 (2011).
20. Jernvall, J., Gilbert, C. C. & Wright, P. C. in *Elwyn Simons: A Search for Origins* (eds Fleagle, J. G. & Gilbert, C. C.) 335–342 (Springer, 2008).
21. Prideaux, G. J. Systematics and evolution of the sthenurine kangaroos. *Univ. Calif. Publ. Geol. Sci.* **146,** 1–622 (2004).
22. Barrett, P. M., McGowan, A. J. & Page, V. Dinosaur diversity and the rock record. *Proc. R. Soc. B* **276,** 2667–2674 (2009).
23. Foote, M. The evolution of morphological diversity. *Annu. Rev. Ecol. Syst.* **28,** 129–152 (1997).
24. Lupia, R., Lidgard, S. & Crane, P. R. Comparing palynological abundance and diversity: implications for biotic replacement during the Cretaceous angiosperm radiation. *Paleobiology* **25,** 305–340 (1999).
25. Feild, T. S. *et al.* Fossil evidence for Cretaceous escalation in angiosperm leaf vein evolution. *Proc. Natl Acad. Sci. USA* **108,** 8363–8366 (2011).
26. Wing, S. L. & Tiffney, B. H. in *The Origins of Angiosperms and Their Biological Consequences* (eds Friis, E.M., Chaloner, W.G. & Crane, P.R.) 203–224 (Cambridge Univ. Press, 1987).
27. Schneider, H. *et al.* Ferns diversified in the shadow of angiosperms. *Nature* **428,** 553–557 (2004).
28. Grimaldi, D. The co-radiations of pollinating insects and angiosperms in the Cretaceous. *Ann. Mo. Bot. Gard.* **86,** 373–406 (1999).
29. Wilson, G. P. Mammalian faunal dynamics during the last 1.8 million years of the Cretaceous in Garfield County, Montana. *J. Mamm. Evol.* **12,** 53–76 (2005).

Supplementary Information is linked to the online version of the paper at www.nature.com/nature.

Acknowledgements We thank museums, institutions and individuals that made specimens available for this study (full list is available in Supplementary Information). Funding was provided by the National Science Foundation, Denver Museum, the University of Washington (G.P.W. and P.D.S.), the Australian Research Council, Monash University (A.R.E.), the Academy of Finland (A.R.E., M.F. and J.J.) and the EU SYNTHESYS program (project GB-TAF-4779) (I.J.C.).

Author Contributions G.P.W., A.R.E., J.J. and M.F. designed the study. G.P.W., A.R.E, I.J.C. and P.D.S. collected and analysed the data. G.P.W., A.R.E. and J.J. wrote the manuscript. G.P.W., A.R.E., I.J.C., P.D.S., M.F. and J.J. discussed results and commented on the manuscript at all stages.

Author Information The three-dimensional scans for this study are deposited in the MorphoBrowser database (http://morphobrowser.biocenter.helsinki.fi/). Reprints and permissions information is available at www.nature.com/reprints. The authors declare no competing financial interests. Readers are welcome to comment on the online version of this article at www.nature.com/nature. Correspondence and requests for materials should be addressed to G.P.W. (gpwilson@u.washington.edu).

doi:10.1038/nature10880

Adaptive Radiation of Multituberculate Mammals Before the Extinction of Dinosaurs

Gregory P. Wilson[1], Alistair R. Evans[2], Ian J. Corfe[3], Peter D. Smits[1,2], Mikael Fortelius[3,4], Jukka Jernvall[3]

[1]Department of Biology, University of Washington, Seattle, WA 98195, USA. [2]School of Biological Sciences, Monash University, VIC 3800, Australia. [3]Developmental Biology Program, Institute of Biotechnology, University of Helsinki, PO Box 56, FIN-00014, Helsinki, Finland. [4]Department of Geosciences and Geography, PO Box 64, University of Helsinki, FIN-00014, Helsinki, Finland.

1. Dental complexity data collection

We scanned lower cheek tooth rows (premolars and molars) of 41 multituberculate genera using a Nextec Hawk three-dimensional (3D) laser scanner at between 10 and 50-µm resolution and in a few cases a Skyscan 1076 micro X-ray computed tomography (CT) at 9-µm resolution and an Alicona Infinite Focus optical microscope at 5-µm resolution. One additional scan from the PaleoView3D database (http://paleoview3d.marshall.edu/) was made on a Laser Design Surveyor RE-810 laser line 3D scanner with a RPS-120 laser probe. 3D scans of cheek tooth rows are deposited in the MorphoBrowser database (http://morphobrowser.biocenter.helsinki.fi/). The

sampled taxa provide broad morphological, phylogenetic, and temporal coverage of the Multituberculata, representing 72% of all multituberculate genera known by lower tooth rows. We focused at the level of genera rather than species under the assumption that intrageneric variation among multituberculates is mostly based on size not gross dental morphology. The sampled cheek tooth rows for each genus are composed of either individual fossil specimens or epoxy casts with complete cheek tooth rows or cheek tooth row composites formed from multiple fossil specimens or epoxy casts of the same species. *Barbatodon* and *Hainina* are exceptions, in which composites were constructed from specimens representing multiple species of each genus. For some genera, more than one cheek tooth row was scanned, representing either multiple individuals of a single species or multiple species from the same genus.

Scan data were digitized, processed, and analyzed as in Evans et al.[18]. The 3D point files were converted into digital elevation models (DEMs) of the cheek tooth rows. To focus on shape apart from size, all cheek tooth rows were scaled to a length of 150 pixel rows. The number of 'tools' on the crown or the 'dental complexity' was approximated by GIS analyses of the full 3D shape of the occlusal surface of the cheek teeth. The specific measure of 'dental complexity' that we used is 'orientation patch count' (OPC). It is calculated by first determining the surface orientation at each pixel on the DEM. Then contiguous pixels that are facing the same cardinal direction (e.g., north, south, southwest) are grouped into patches. The number of these 'patches' is the 'orientation patch count' or the OPC. To reduce the effect of a specific tooth orientation, the OPC calculation was repeated eight times at rotations of multiples of 5.625º and the mean of these

repetitions is used (OPCR). For the dataset of Evans et al.[18], OPC and OPCR are highly correlated (adjusted $R^2 > 0.98$ for both upper and lower), with the average deviation of OPC from OPCR being 3.00%. The same analyses in Evans et al.[18] were re-run on the OPCR data and no differences were found in recorded patterns (Supplementary Table 6).

Although degree of wear among specimens varies and despite studies having shown that specific functional features may be modified by tooth wear[30], general topographic measures tend to be more stable. This suggests that higher-level patterns, like OPC, are relatively robust to wear[31]. Specifically in the case of OPC, all slopes irrespective of their steepness are included in calculations; hence even worn cusp features are typically tabulated. Nevertheless, we excluded fossil specimens with excessive tooth wear or post-mortem abrasion. Specimens with moderate/heavy wear that were included in the analysis are in boldface in Supplementary Table 1. When we excluded those specimens with moderate/heavy wear from the analyses, the pattern of results remained the same. Note that the use of worn specimens typically underestimates OPC and thus decreases the amount of herbivory inferred.

To examine intraspecific variation of OPC, the coefficient of variation (SD/Mean) for 18 specimens of *Apodemus flavicollis* unworn lower tooth rows was 8.56% (mean $\pm$ SD: 216.85 $\pm$ 18.56). The relative standard error ((SD/$\sqrt{n}$)/Mean) is 2%.

To test for the compatibility of data from different scanning systems, two multituberculate tooth row casts (*Meniscoessus robustus* UCMP 107405, *Parikimys carpenteri* DMNH 52224) were scanned with a Nextec Hawk point laser scanner (University of Helsinki), Skyscan 1076 MicroCT scanner (University of Washington,

Seattle), and a Laser Design Surveyor DS2025 laser line scanner (Monash University, Melbourne) at 10 µm resolution (Supplementary Figures 9 and 10). The relative standard error of the measurements of OPC values for the tooth rows, downsampled to 150 data rows, was less than 3.1% (Supplementary Table 7). We were unable to include the Alicona Infinite Focus optical microscope in this comparison. Nevertheless, only two Late Jurassic specimens were scanned using this machine. When they are removed from the dataset, there is no effect on the major results of the study.

For genera with more than one sampled cheek tooth row, OPC values varied by no more than 15% of the mean OPC. For these genera, we used the mean OPC value. The specimens used in each of our sampled cheek tooth rows and their OPC values are listed in Supplementary Table 1 and plotted in Fig. 2a as solid horizontal lines, lengths of which correspond to the temporal range of the genus or uncertainties in the age of the fossil localities. Resolution of temporal range data varies from geologic ages to land-mammal ages constrained by radiometric ages. We gratefully acknowledge the museums and institutions listed in Supplementary Table 1, and we would also like to thank the individuals that made these specimens, casts, and scans available: Zofia Kielan-Jaworowska, Dave Krause, Gregg Gunnell, Philip Gingerich, Toni Culver, Jaelyn Eberle, Logan Ivy, William A. Clemens, Patricia Holroyd, Matthew Carrano, Michael Brett-Surman, Nicholas D. Pyenson, Richard C. Fox, Rich Cifelli, Brian Davis, Meng Jin, Ivy Rutzky, Douglas Boyer, Ruth O'Leary, Zoltan Csiki, Thomas Martin, Aisling Farrell, Luis Chiappe, Guillermo Rougier, Suzanne Strait, Jack Horner, Phillipa Brewer, and Jerry Hooker; Bryan Small for cast preparation; William Sanders for specimen

preparation; and Suzanne Strait, Douglas Boyer, Norman Macleod, Jonathan Krieger, Murat Maga, Casey Self, Abby Vander Linden, and Timothy Cox for help with scan data.

To compensate for the relatively poor fossil record from the Late Jurassic and Early Cretaceous (155–100 Myr ago), we developed formulae to estimate OPC values that are based on the positive correlation of OPC and the proportional length of the lower molars in the cheek tooth row ([length of m1 + m2]:[length of all lower premolars]) of sampled multituberculates (Supplementary Fig. 1; $r = 0.750$, $p < 0.0001$, $n = 40$) and the ratio of the lower first molar to the lower fourth premolar (length of m1:length of p4) (Supplementary Fig. 2; $r = 0.711$, $p < 0.0001$, $n = 40$). The resulting estimated OPC values for Late Jurassic and Early Cretaceous taxa (dashed lines in Fig. 2a; Supplementary Table 2) fall within or close to the range of measured OPC values for this interval, suggesting that the pattern for this interval is robust to gaps in the sampling. In Fig. 2a, mean and standard deviation of OPC were calculated for 5-Myr bins, except the poorly sampled Early Cretaceous 136–131 Myr bin. OPC values for dietary classes in extant rodents and carnivorans[18] were mapped on Fig. 2a. Though there is some overlap in dietary classes, lower tooth row OPC values between 60 and 110 include mostly carnivores, between 110 and 160 mostly animal-dominated omnivores, between 160 and 200 mostly plant-dominated omnivores, and above 200 mostly herbivores.

2. Generic richness data collection

Patterns of generic richness provide a view of taxonomic diversification that can be decoupled from morphological diversification[23]. Taxonomic and temporal range data

were compiled from the most recent compendia[3,11,32] and primary literature available up to November 16, 2010. We standardized temporal ranges to the recent Geologic Time Scale of Gradstein[33]. Taxonomic and temporal range data are in Supplementary Table 3. Richness was evaluated at the level of genera not species under the assumption that genera provide a more consistent record of long-term trends in taxonomic richness than more volatile patterns recorded at the species level. The number of described paulchoffatiid multituberculate genera from the Late Jurassic Guimarota fauna[109] is likely artificially inflated: some named taxa are based entirely on upper dentition and may belong to named taxa that are based entirely on lower dentition and vice versa[3]. To adjust for this, we removed six genera that were based entirely on upper dentitions. The data were partitioned into 5-Myr bins. Although partitioning the data into smaller bins would produce higher temporal resolution patterns, low sampling intensity for some intervals and poor age control for some taxa made that impractical. We placed the lower boundary of the first bin at 171 Myr ago so as to have the desired effect of placing a later bin boundary at the K-Pg boundary (ca. 66 Myr ago) rather than having it span this temporal boundary and associated mass extinction event. Whenever the lower temporal range of a taxon fell on an upper bound for a bin, it was counted in the younger bin. For example, the temporal range of *Acheronodon* is 66–60 Myr ago and was thus counted in the 66–61 Myr bin and the 61–56 Myr bin but not the 71–66 Myr bin. The same logic was applied to the upper temporal range of a taxon that fell on a lower bound for a bin. The intensity of mammalian fossil sampling varies through the geologic time interval of this study (171–31 Myr ago) as a result of research emphases and availability of fossil-bearing

exposures. The patterns of generic richness should thus be viewed as long-term trends rather than placing too much emphasis on individual fluctuations. We excluded a 5-Myr temporal bin from the analyses because of notably poor sampling; the 136–131 Myr bin included only one recorded multituberculate genus. In Figure 2a-c, we spanned this sampling gap with a dashed line connecting the data points on either side, the 141–136 Myr bin and the 131–126 Myr bin. Generic richness data are in Supplementary Table 4.

3. Body mass data collection

Body size provides a second measure of ecomorphological diversification and is correlated with a variety of life history traits in extant mammals[34]. Estimates of multituberculate body mass were initially calculated based on a formula presented in Legendre[35] that was derived from a database of extant therian mammals that includes rodents, primates, artiodactyls, perissodactyls, lipotyphlans, chiropterans, carnivorans, and marsupials. The formula is as follows: LN (body mass) = 1.827 * LN (lower m1 area) + 1.81. Because multituberculates are phylogenetically outside of Theria (e.g., ref. 3), application of this formula to multituberculates requires justification. McDermott et al.[36] applied this formula, along with other formulae based on cranial and postcranial measurements, to multituberculates. They found that the generalized formula of Legendre[35] produced estimates convergent with estimates from other formulae, and thus deemed it reasonable to apply this formula to estimate multituberculate body mass. We estimated body mass for multituberculate species rather than genera because congeneric species are often discriminated from each other based on dental dimensions or other size

correlates; generic-level body mass estimates would overlook this variation. We calculated lower m1 area for 156 multituberculate species based on m1 length and width measurements that were compiled from the primary literature and our own measurements using a Leica MZ9.5 binocular dissecting microscope and custom measuring stage that has the capability of reading to the nearest 0.001 mm. When more than one measurement was available for a taxon, mean values were used to calculate lower m1 area. In a few cases measurements were not published and casts or specimens were not available, so estimates were made from published figures.

Body mass estimates based on lower m1 area appear reasonable for small-bodied multituberculates but are larger than expected for large-bodied multituberculates (e.g., *Taeniolabis taoensis* body mass estimate > 100 kg); this implies that scaling of lower m1 area to body mass differs in multituberculates and the reference group (Theria). Because the rodent skull and body plan is similar in appearance, rodents have often been suggested as a suitable analog for multituberculates. On this basis, we investigated predictive formulae that use modern rodents as a reference group[37-39]. From the supplementary data of ref. 38, we generated a bivariate plot of skull length (SL) vs. upper tooth row length (UTRL) of modern rodents (n = 35) onto which we plotted the same measurements available in 10 multituberculate taxa (Supplementary Fig. 3). For multituberculates, UTRL is the sum of the upper P4, M1, and M2 lengths. More broadly among mammals, SL is viewed as a more reliable predictor of body mass than molar dimensions[40] and has been used to estimate body mass in Mesozoic mammaliaforms[41]. Derivatives of SL, such as mandible length, have also been successfully used to estimate

body mass in non-therian Mesozoic mammals[42]. Unfortunately few multituberculate taxa are known from complete skulls. SL measurements for 10 multituberculate taxa, including the large-bodied *Taeniolabis taoensis*, are mostly based on specimens from the Campanian of Mongolia and Paleocene of North America. We concluded that UTRL and SL have a similar scaling relationship within rodents and multituberculates, because the multituberculate data plotted among the rodent data. Thus, rodents are an appropriate reference group for estimating body mass in multituberculates.

To further constrain the nature of discrepancy between estimates from the general therian formula[35] and rodent formulae[37,39], we plotted body mass estimates of multituberculates based on lower m1 area[35] against estimates from other anatomical elements (SL[39], UTRL[39], lower tooth row length[37]) available for 10 to 13 multituberculate taxa. As estimates based on lower m1 area exceeded ca. 1 kg they became increasingly larger than estimates based on other anatomical elements. Because SL takes into account a greater proportion of the animal's total length than either UTRL or LTRL, we would expect body mass estimates based on SL to be more accurate than those based on UTRL or LTRL. Thus, whenever possible, we used SL to estimate body mass according to the formula[39]: Log (body mass) = 3.488 * (Log SL) – 3.332. Unfortunately, SL is not as widely available as UTRL or LTRL. For large-bodied taxa, LTRL estimates were less than expected based on skull length. UTRL estimates were consistently greater than expected based on skull length (Supplementary Fig. 4d). Thus, for species without skull length data, we developed a regression formula to predict the SL body mass estimate from the lower m1 area body mass estimate, the most readily available estimate (see

Supplementary Fig. 5). This approach provides more conservative estimates of body mass than provided from UTRL, LTRL, and m1 area formulae. Estimates for the smallest multituberculates (under 100 g based on m1 area formula) are slightly greater when using the m1-SL regression formula and estimates for remaining multituberculates (over 100g based on the m1 area formula) are slightly less than estimates from UTRL or m1 area formulae, producing a more compressed body size distribution overall. Supplementary Table 5 includes lower m1 area, SL, predicted body mass, and sources for measurements. In Figure 2c, body mass estimates from Supplementary Table 5 were plotted as horizontal lines, lengths of which correspond to the temporal range of the species. We calculated geometric mean and standard deviation of body masses for each 5-Myr bin, except the Early Cretaceous 136–131 Myr bin. Nevertheless, because only ten of the 156 multituberculate body size estimates are based on skulls, which provide a more reliable basis to estimate body size than teeth alone, the body size trends should be considered approximate.

4. Correlation of estimated body mass and OPC

Because of the relationship between metabolic rate and body size in mammals[43-47], small-bodied mammals often cannot subsist on a strictly herbivorous diet of leaves low in nutritional value[48-50]. Small-bodied mammals generally require a diet of high-energy content foods, such as fruits and insects. To test whether dental complexity as measured by OPC followed this pattern, we investigated the correlation of OPC and estimated body mass. Because OPC values in the sample are skewed toward higher

values, we log transformed the data. We found that ln(body mass) and ln(OPC) are strongly correlated in the sampled multituberculates (Pearson correlation coefficient = 0.672, $p < 0.01$, $n = 40$; Supplementary Fig. 6) and thus generally consistent with this claim; smaller-bodied multituberculates tend to have low OPC values corresponding to carnivorous or animal-dominated omnivorous diets, whereas larger-bodied multituberculates have high OPC values indicative of herbivorous diets with a greater proportion of stems and leaves. However, as in modern mammals, there are exceptions to this general pattern. The small-bodied multituberculate *Chulsanbaatar vulgaris* (13.3 g) has a high dental complexity (OPC 171), whereas the larger-bodied *Neoliotomus ultimus* (3.84 kg) has a low dental complexity (OPC 130).

5. Resampling routine and permutation simulation

To investigate whether the temporal patterns of OPC and body mass are due to differences in sampling, OPC and body mass values were permuted among taxa. OPC was randomized at the generic level, while body mass was randomized at the species level. Both measures were natural log transformed. Data were binned in 5-Myr durations where all taxa that occur within that bin were sampled. As described above, taxa that have their first appearance at the bottom of a bin were excluded. The K-Pg boundary (66 Myr ago) was used as the date from which bin values were calculated. In both cases, the age range of each measured taxon was preserved while the measurement information was randomly assigned to an age range. Because the desired alpha, or level of significance, was set at 0.05 and to reduce volatility[51], this procedure was repeated 5000 times,

creating 5000 randomized mean values for each bin. All simulations were done in the R programming environment[52]. The random seed was set at the beginning of the simulation.

In Supplementary Figures 7 and 8 (OPC and body mass, respectively), the observed mean in every bin was plotted (black line) versus time and then compared to the 2.5 and 97.5 percentiles of the resampling distribution (dashed blue line). Significant difference is determined as when the observed mean value falls outside of this two-tailed confidence interval based on the resampled distribution (2.5–97.5 percentile).

Observed OPC values fall outside of the two-tailed confidence interval in four bins (156–151, 146–141, 141–136 and 76–71 Myr ago). For 156–151, 146–141 and 141–136 Myr ago, the observed mean is significantly lower than the randomized distribution, and from 76–71 Myr ago the observed mean is significantly greater (Supplementary Fig. 7). The observed body mass values fall outside of the two-tailed confidence interval in four bins (146–141, 141–136, 101–96 and 71–66 Myr ago). In the first three of these bins, the observed mean is significantly lower than the randomized distribution, and in the 71–66 Myr bin the observed mean is significantly greater (Supplementary Fig. 8). In all other cases, the observed mean is not statistically different from the randomized distribution.

Lastly, we would like to acknowledge L. Berg, J. Calede, M. Chen, D. Demar, Jr., S. Donohue, N. Pyenson, C. Sidor, C. Strömberg, and J. Wilson for reviews and comments on the manuscript.

Supplementary Figure 1. Least-squares linear regression of OPC and the natural log of the lower molars to premolars length ratio. R = 0.750, p < 0.0001, n = 40. Predictive equation: OPC = 121.44 + 57.20*(ln molars:premolars length ratio).

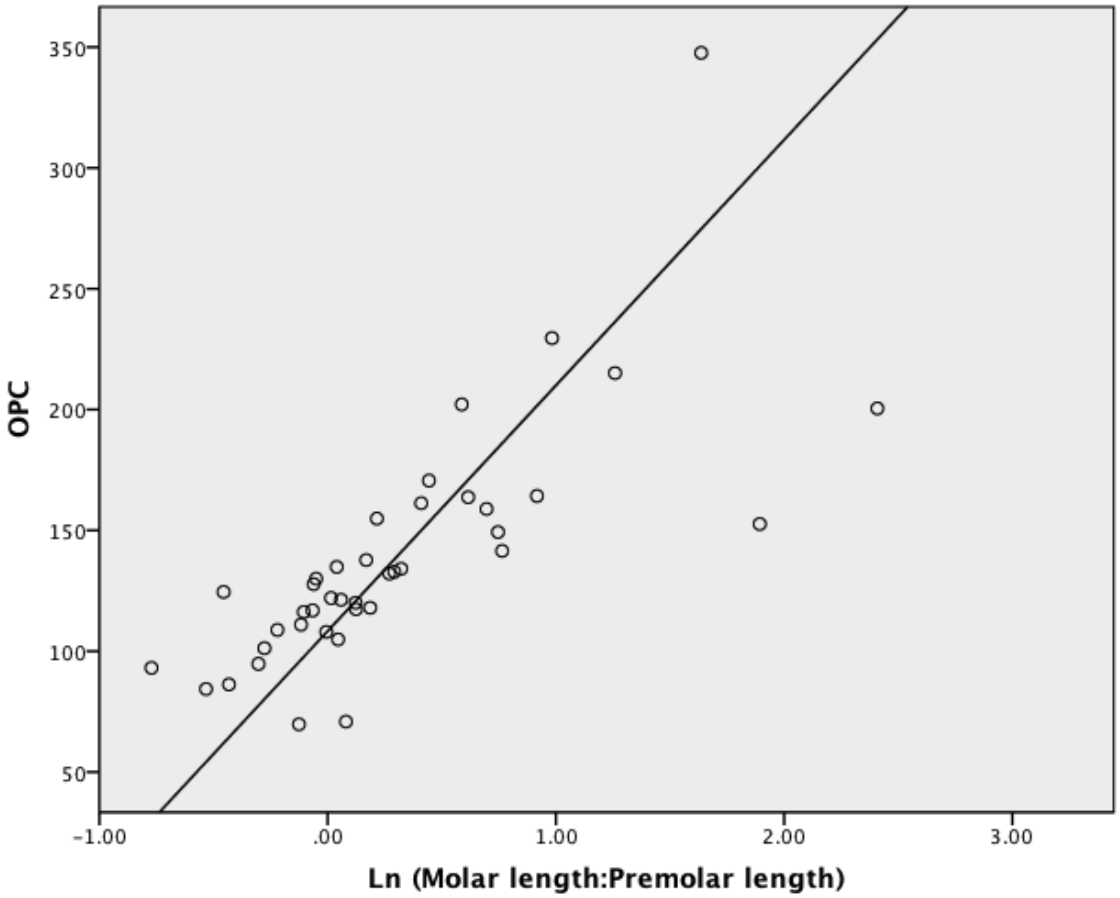

Supplementary Figure 2. Least-squares linear regression of OPC and the natural log of lower first molar (m1) to lower fourth premolar (p4) length ratio. R = 0.711, $p < 0.0001$, n = 40. Predictive equation: OPC = 147.15 + 62.48*(ln m1:p4 length ratio).

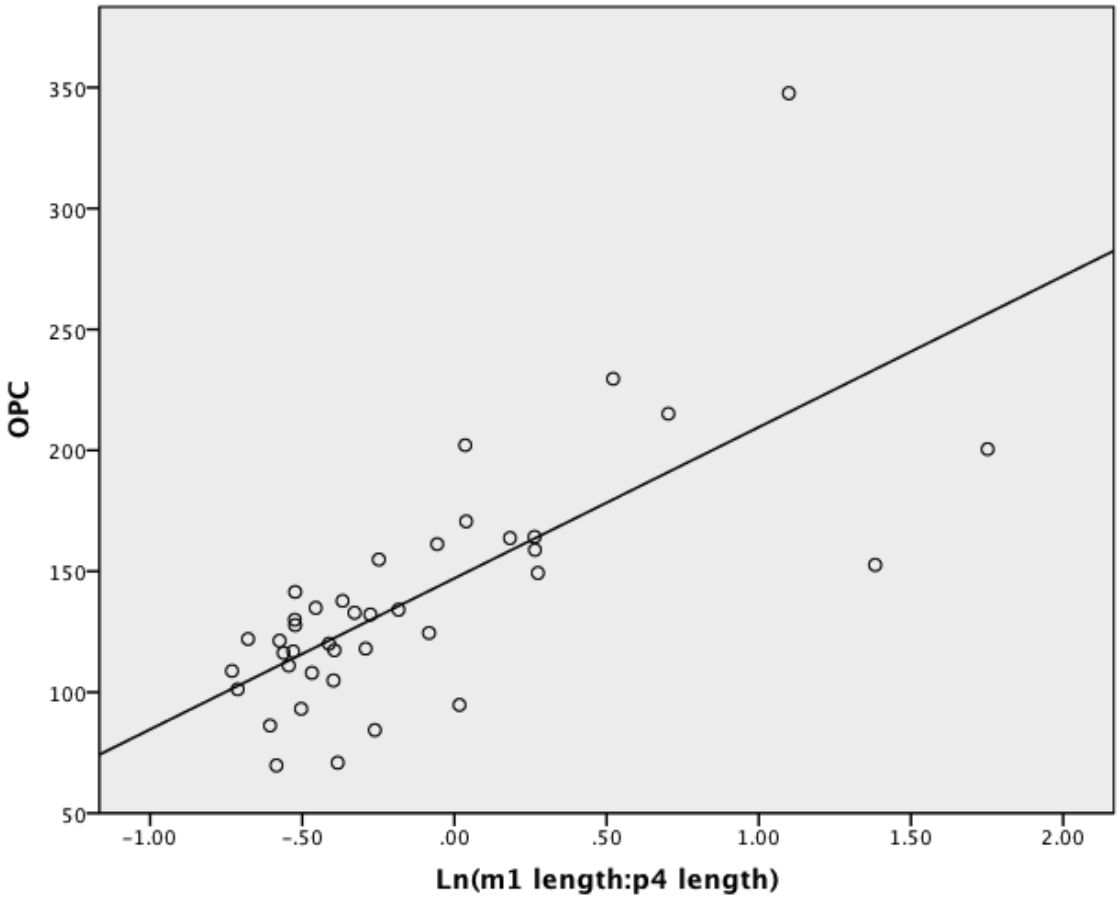

Supplementary Figure 3. Plot of skull length (SL) vs. upper tooth row length (UTRL) for rodent sample (open circles, n = 35) from ref. 38 and multituberculates (filled squares, n =35) from this study.

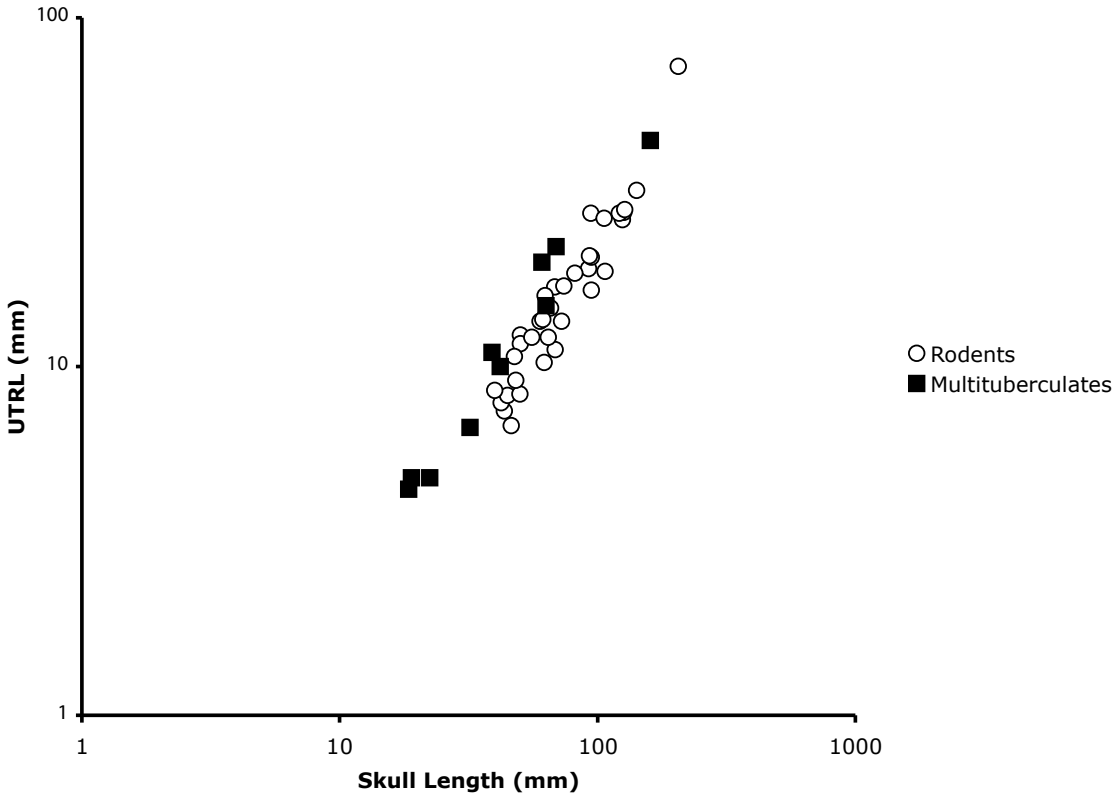

Supplementary Figure 4. Plots of body mass estimates based on lower first molar (m1) area[35] vs. (**a**) body mass estimates from upper tooth row length (UTRL[39], n = 12), (**b**) lower tooth row length (LTRL[37], n = 11), and (**c**) skull length (skull L[39], n = 10) for select multituberculate species; and (**d**) estimates from skull length vs. UTRL (n = 10). Scale in kilograms. Dashed line is $y=x$.

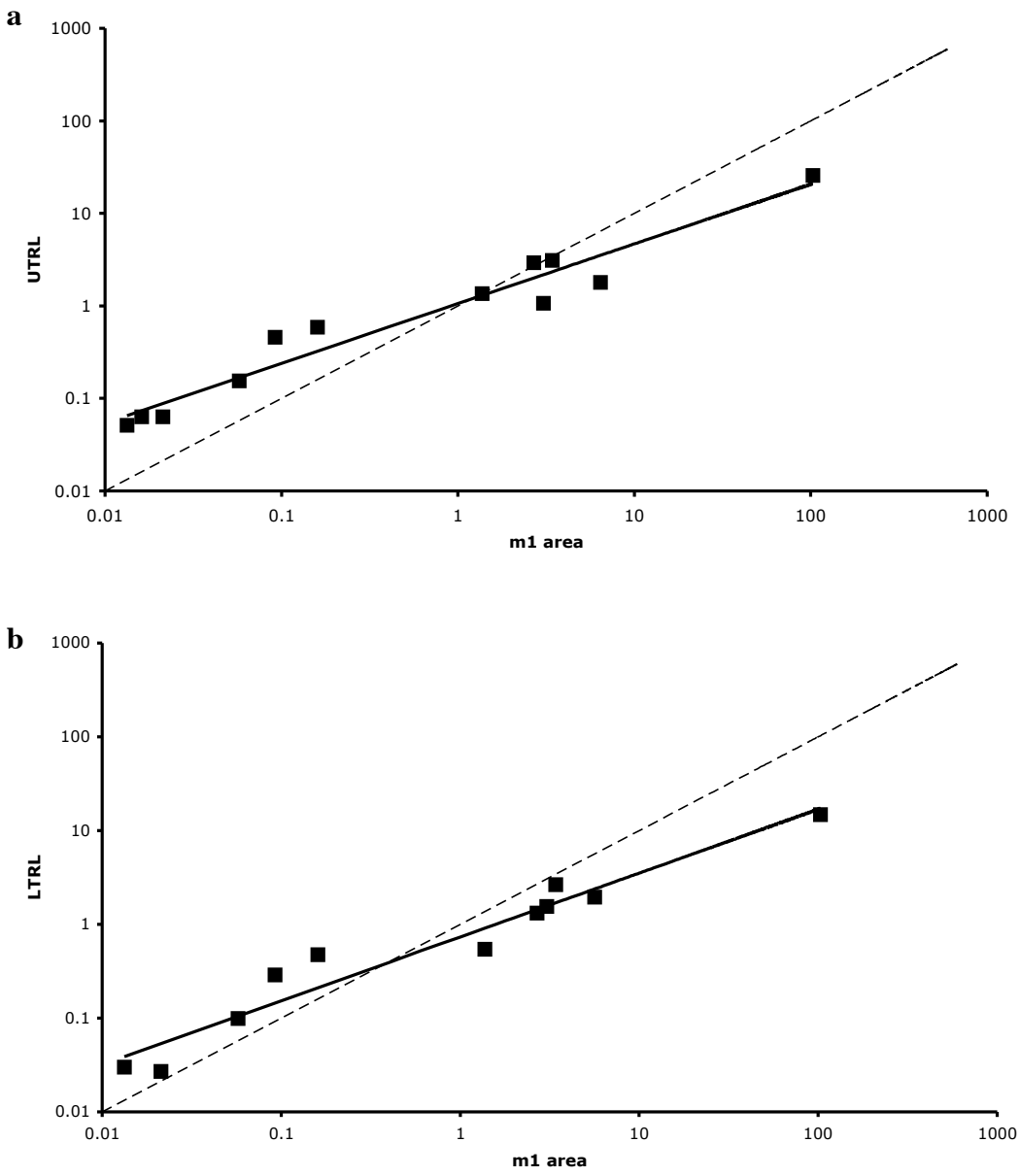

c

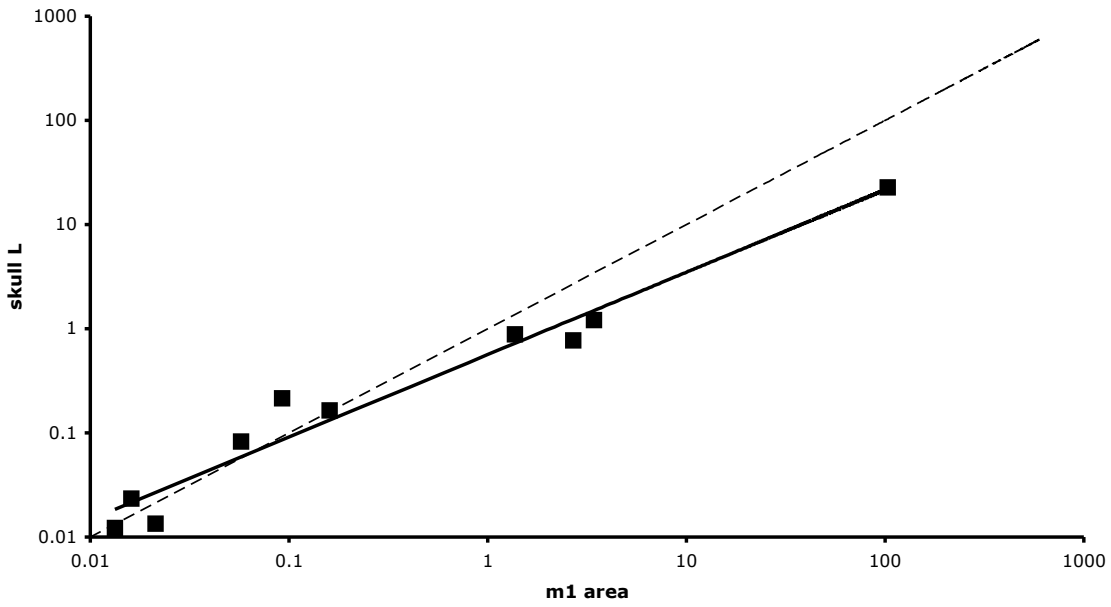
1000
100
10
1
0.1
0.01
skull L
0.01
0.1
1
10
100
1000
m1 area

d

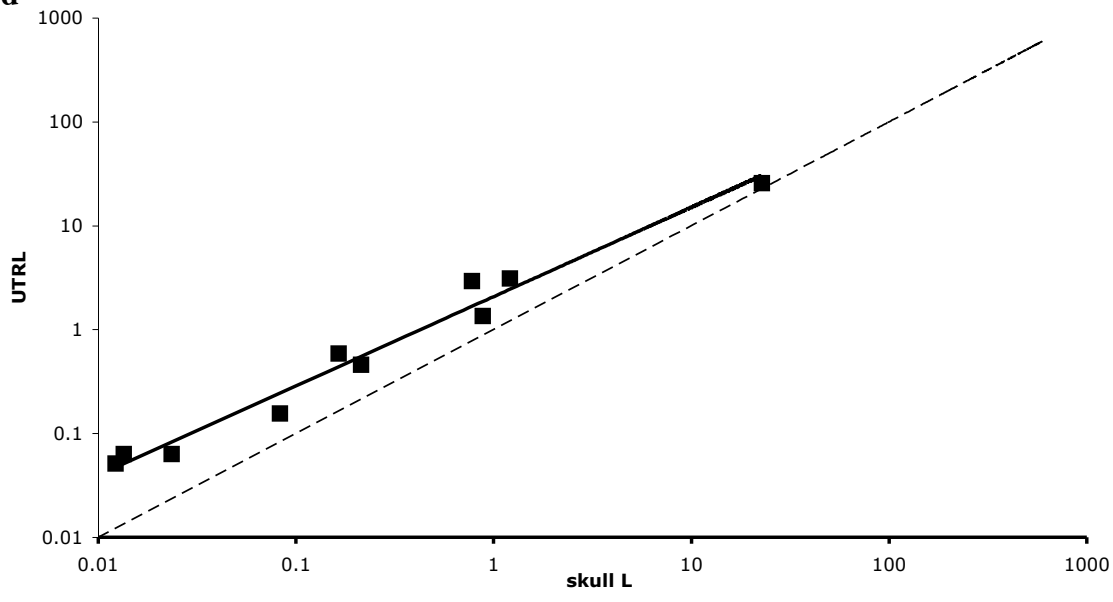
1000
100
10
1
0.1
0.01
UTRL
0.01
0.1
1
10
100
1000
skull L

Supplementary Figure 5. Least-squares linear regression of the natural log of body mass estimated from lower first molar (m1) area[35] and the natural log of body mass estimated from the skull length (SL)[39] for select multituberculate species. R = 0.980, $p < 0.0001$, n = 10. Predictive equation: SL body mass estimate = 0.87 + 0.79*(ln m1 body mass estimate).

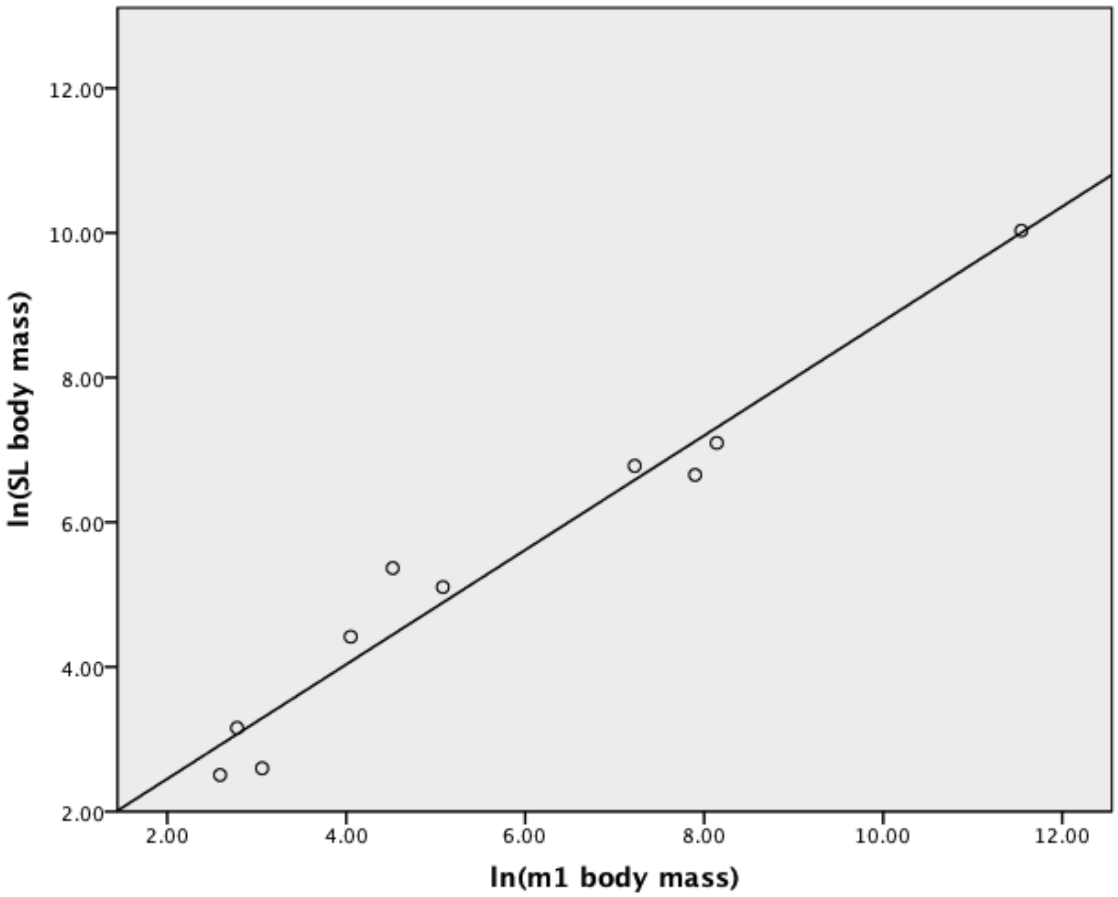

Supplementary Figure 6. Bivariate plot of the natural log of body mass estimates and natural log of OPC values for sampled multituberculates. Pearson correlation coefficient = 0.683, $p < 0.01$, $n = 40$.

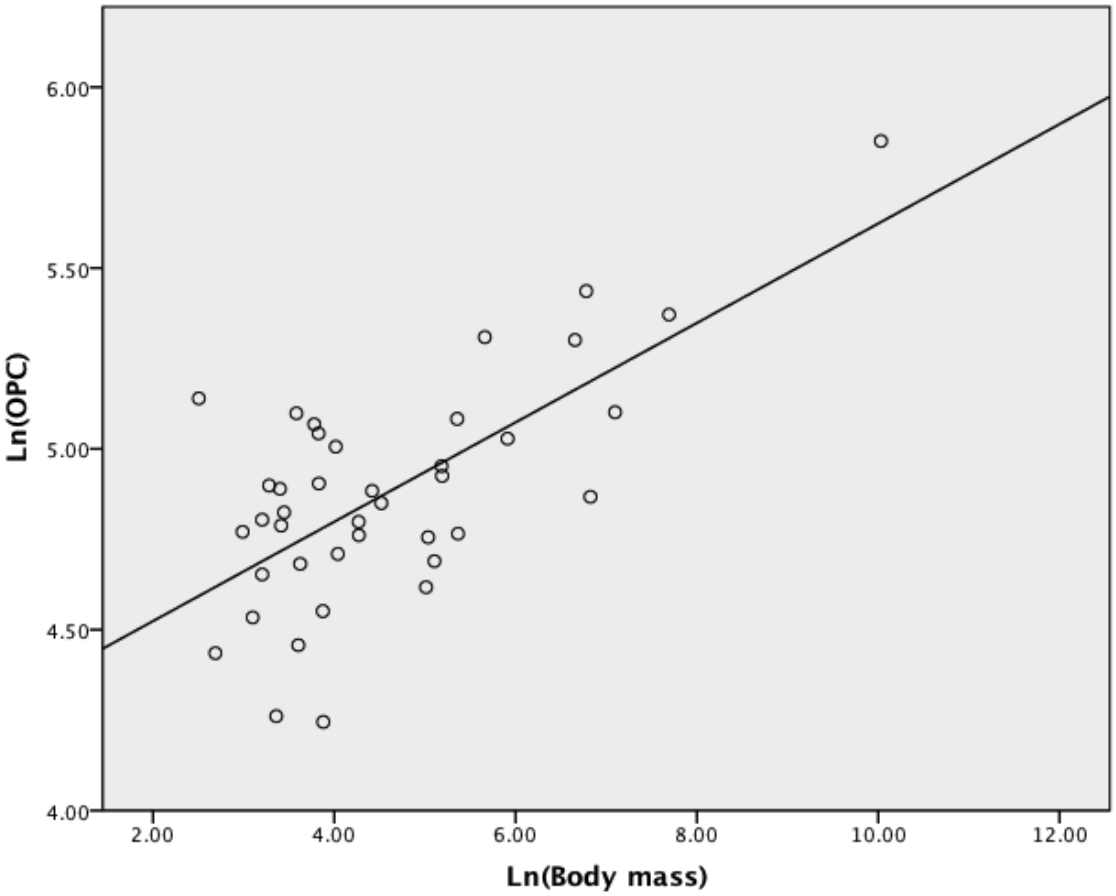

Supplementary Figure 7. Plot of natural log of OPC resampling simulation with mean (blue line) and 95% confidence limits (blue dashed lines) shown along with the mean of the natural log of the observed OPC (black line).

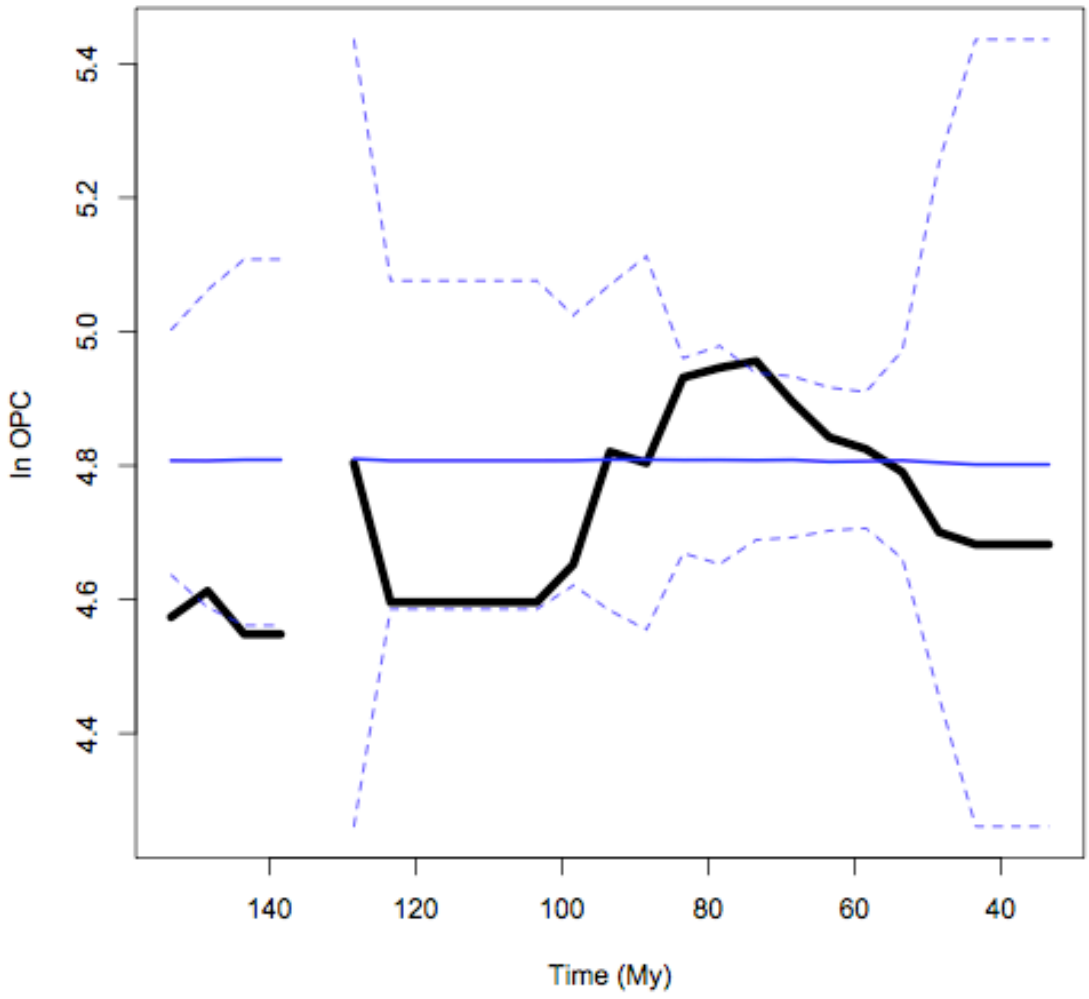

Supplementary Figure 8. Plot of natural log of body mass resampling simulation with mean (blue line) and 95% confidence limits (blue dashed lines) shown along with the mean of the natural log of observed body mass (black line).

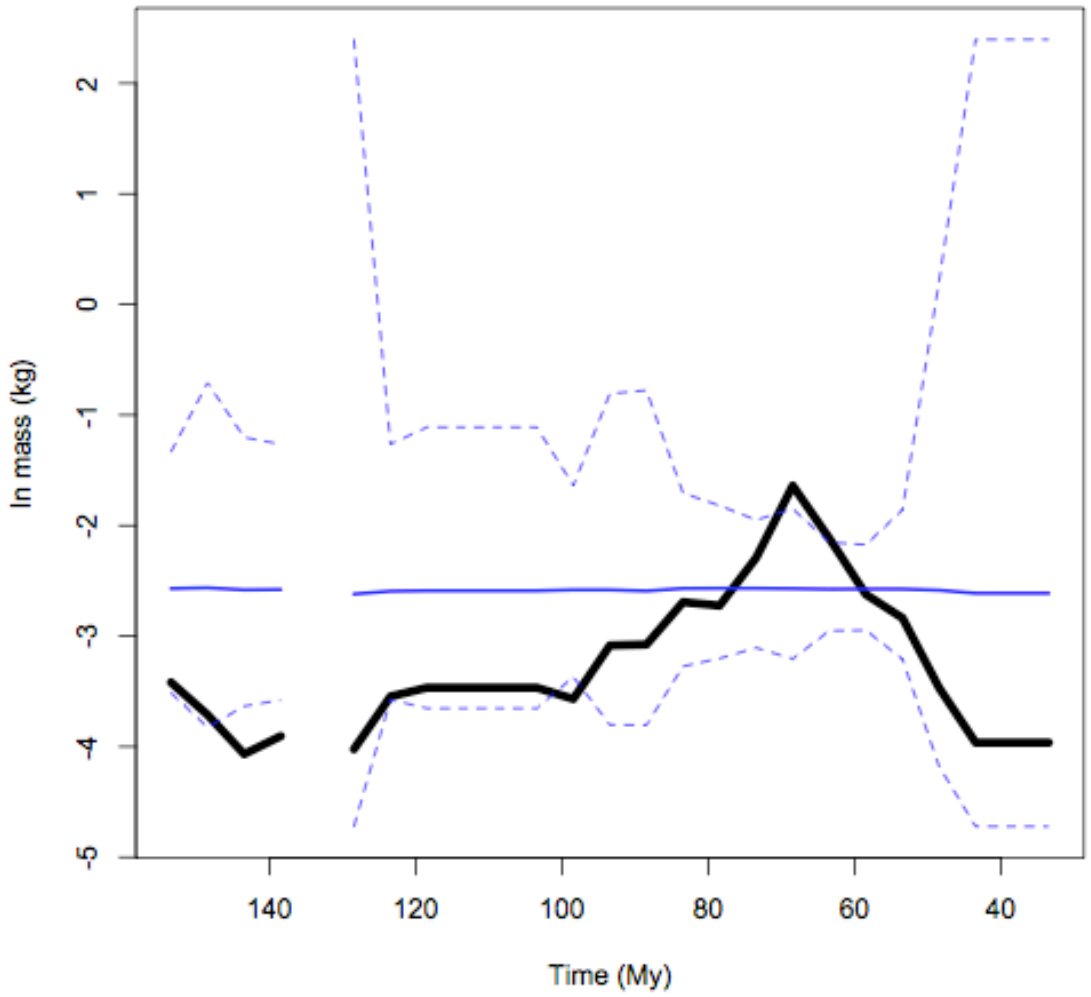

Supplementary Figure 9. Comparisons of surfaces from three scanners scanning the same cast (*Meniscoessus robustus* UCMP 107405), illustrating both the full resolution surface and downsampled to 150 rows, as used in OPC analysis.

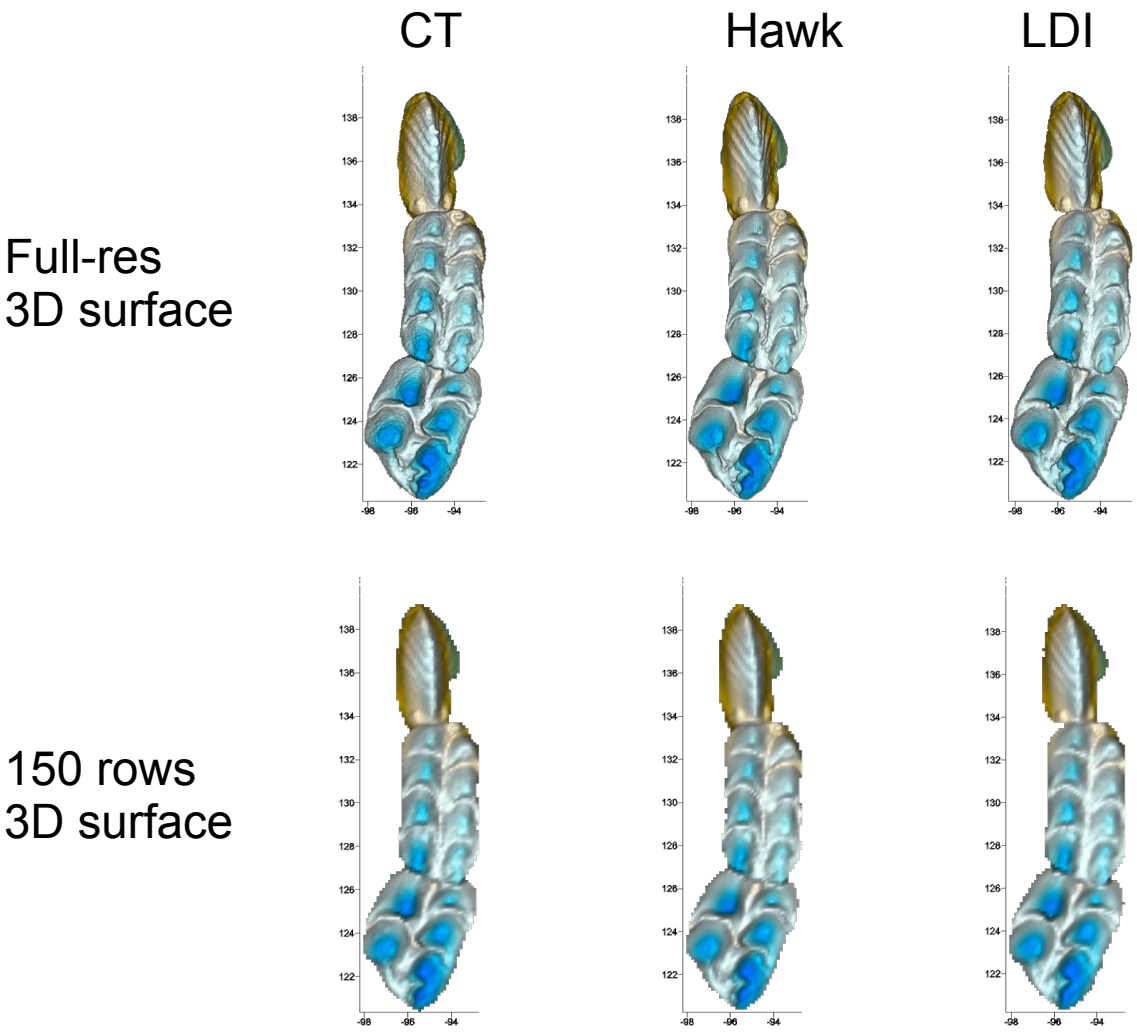

Supplementary Figure 10. Comparisons of surfaces from three scanners scanning the same cast (*Parikimys carpenteri* DMNH 52224), illustrating both the full resolution surface and downsampled to 150 rows, as used in OPC analysis.

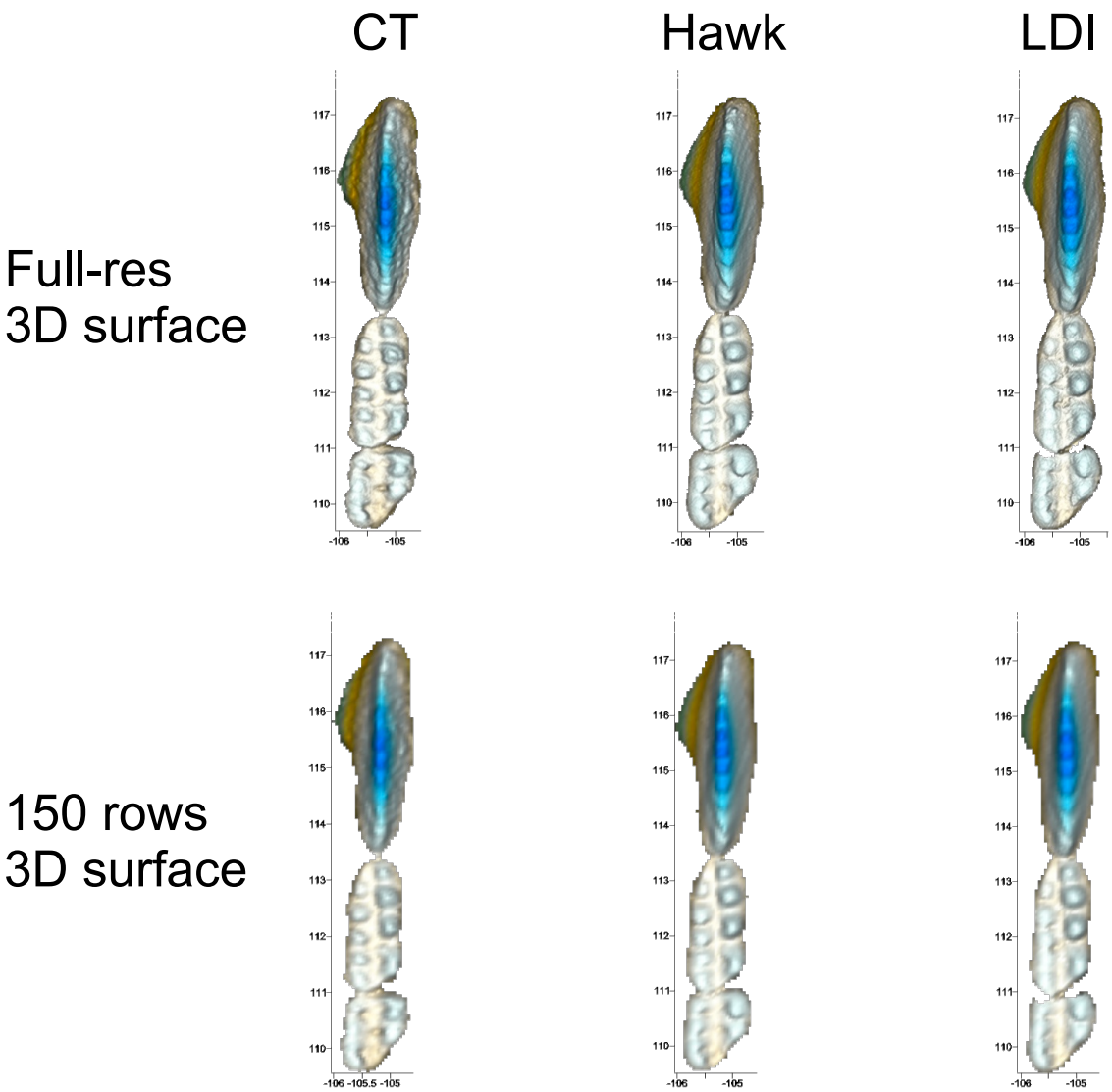

Supplementary Table 1. Multituberculate specimens scanned, digitized, processed, and analyzed for OPC measurement. Each row represents a complete cheek tooth row, either from a single specimen or a composite reconstructed from multiple specimens, that was sampled in this study. OPC species is the average OPC value if the species has more than one sampled cheek tooth row. OPC genus is the average OPC value if the genus has more than one sampled cheek tooth row. Specimens in bold have moderate/heavy wear.

Species	Specimen #	OPC	OPC species	OPC genus
Acheronodon vossae	UALVP 24544, 42798, 24578	163.75	163.75	163.75
Allocosmodon woodi	**UALVP 40494**	154.875	154.875	154.875
Anconodon cochranensis	USNM 9765	111	111	111
Baiotomeus douglassi	USNM V9795	116.25	116.25	116.25
Barbatodon transylvanicus, B. sp. indet.	**FGGUB R.1635, 1623**	141.5	141.5	141.5
Bolodon osborni	BMNH 48399, DORCM GS2, 206	93.125	93.125	93.125
Bryceomys fumosus	MNA V7476, V6298, V6765	114	114	120.0625
Bryceomys intermedius	OMNH 34005, 33001, 26626	126.125	126.125	-
Catopsalis alexanderi	**UCM 34979**	215.125	215.125	215.125
Catopsbaatar catopsaloides	PM 120/107	202.625	202.625	202.625

Species	Specimen #	OPC	OPC species	OPC genus
Cedaromys bestia	OMNH 26636, 25752, 33186	122	122	121.3125
Cedaromys parvus	OMNH 32987, 25750, 25760	120.625	120.625	-
Chulsanbaatar vulgaris	ZPAL MgM-I/108	170.625	170.625	170.625
Cimexomys judithae	MOR 302	134.125	134.125	134.125
Cimolodon nitidus	AMNH 57860	137.75	137.75	137.75
Cimolomys gracilis	UCMP 51514, 51552, 51669	202.125	202.125	202.125
Ctenacodon serratus	YPM 11832	84.375	84.375	84.375
Dakotamys malcolmi	MNA V6056, V6384, V6488	132.875	132.875	132.875
Ectypodus musculus	AMNH 17391	100.625	100.625	108
Ectypodus tardus	PU 13265	115.375	115.375	-
Eobaatar magnus	PIN 3101/60, PIN 3101/53	122	122	122
Glirodon grandis	LACM 120452	124.5	124.5	124.5
Hainina belgica, H. godfriauxi	HIN 16-16 60-1, HIN 17-17 70-2, HIN 17-17 70-3	116.5	116.5	116.5
Kimbetohia mziae	UCM 38858	116.875	116.875	116.875
Kryptobaatar dashzevegi	GI-PST 8-2	132.125	132.125	132.125
Lambdopsalis bulla	**IVPP V7152.17**	200.5	200.5	200.5
Meketibolodon robustus	**IPFUB Gui Mam 89/76**	94.75	94.75	94.75

Species	Specimen #	OPC	OPC species	OPC genus
Meniscoessus robustus	UCMP 107405	164.25	164.25	164.25
Mesodma archibaldi	MNA V7531	114.75	114.75	118
Mesodma pygmaea	AMNH 35298	121.25	121.25	-
Microcosmodon conus	**PU 22316**	158.25	158.875	158.875
Microcosmodon conus	**UALVP 42711**	159.5	-	-
Mimetodon silberlingi	**USNM 9798**	70.875	70.875	70.875
Nemegtbaatar gobiensis	ZPAL MgM-I/81	117.375	117.375	117.375
Neoliotomus ultimus	UW 10433, 10428, 6577, 10430	130	130	130
Neoplagiaulax hunteri	UALVP 9955, 9787, 11977	69.25	69.25	69.25
Parectypodus trovessartianus	AMNH 3026	127.75	127.75	127.75
Parikimys carpenteri	DMNH 52224	134.875	134.875	134.875
Pentacosmodon bowensis	UALVP 42806, 24650, 42800	160	160	149.3125
Pentacosmodon pronus	MCZ 20066	138.625	138.625	-
Plagiaulax becklesii	BMNH 47731, 47733	86.25	86.25	86.25
Prionessus lucifer	AMNH 21731	152.625	152.625	152.625
Prochetodon taxus	UM 71311	101.25	101.25	101.25
Ptilodus kummae	UALVP 10912, 9001, 10253	106.75	106.75	108.8125
Ptilodus montanus	USNM 6076	110.875	110.875	-

Species	Specimen #	OPC	OPC species	OPC genus
Stygimys kuszmauli	UCMP 92525, 92528, 133000	161.25	161.25	161.25
Taeniolabis taoensis	NMMNH P-8631	347.625	347.625	347.625
Xyronomys robinsoni	UCM 34975	104.875	104.875	104.875

Museum abbreviations: AMNH, American Museum of Natural History; BMNH, British Museum of Natural History; DMNH, Denver Museum of Nature & Science; FGGUB, Faculty of Geology and Geophysics, University of Bucharest, Romania; GI-PST and PM, Mongolian Academy of Sciences; HIN, Paleontology collections of l'Université des Sciences et Techniques de Montpellier, France; IPFUB, Instituts für Paläontologie der Freien Universität; IVPP, Institute of Vertebrate Paleontology and Paleoanthropology; LACM, Los Angeles County Museum; MCZ, Harvard University Museum of Comparative Zoology; MNA, Museum of Northern Arizona; MOR, Museum of the Rockies; NMMNH, New Mexico Museum of Natural History; OMNH, Oklahoma Museum of Natural History; PIN, Paleontological Institute of the Russian Academy of Sciences; PU, Princeton University collection held by Yale University Peabody Museum; UALVP, University of Alberta Vertebrate Paleontology collections; UCM, University of Colorado Museum; UCMP, University of California Museum of Paleontology; UM, University of Michigan Museum of Paleontology; USNM, United States National Museum; UW, University of Wyoming Geological Museum; YPM, Yale University Peabody Museum; ZPAL, Polish Academy of Sciences, Institute of Paleobiology.

Supplementary Table 2. Estimated OPC values for multituberculate species unavailable for this study. Predictive formulae are based on the regression analyses in Supplementary Figs. 1, 2.

Species	ln (molar L:premolar L)	ln (m1 L:p4 L)	estimated OPC
Arginbaatar dimitrievae	-0.775	-	77.13
Buginbaatar transaltaiensis	0.833	-	169.08
Djadochtatherium matthewi	0.608	-	156.23
Essonodon browni	0.221	-	134.11
Eucosmodon americanus	-	-0.638	107.28
Guimarotodon leiriensis	-0.626	-	85.62
Heishanobaatar triangulus	-0.317	-	103.30
Iberodon quadrituberculatus	0.057	-	124.71
Kamptobaatar kuczynskii	-0.288	-	104.98
Krauseia clemensi	0.037	-	123.54
Kuehneodon dietrichi	-0.310	-	103.70

Species	ln (molar L:premolar L)	ln (m1 L:p4 L)	estimated OPC
Liaobaatar changi	-0.499	-	92.88
Liotomus marshi	-0.461	-	95.09
Mesodmops dawsonae	-0.164	-	112.06
Nessovbaatar multicostatus	-0.121	-	114.49
Nidimys occultus	-	-0.300	128.41
Paracimexomys priscus	0.159	-	130.55
Paulchoffatia delgadoi	-0.510	-	92.25
Pinheirodon pygmaeus	-0.734	-	79.44
Psalodon marshi	-0.525	-	91.40
Sinobaatar xiei	-0.274	-	105.75
Sloanbaatar mirabilis	-	-0.463	118.24
Uzbekbaatar wardi	-	-0.591	110.21
Zofiabaatar pulcher	-	-0.685	104.32

Supplementary Table 3. Multituberculate genera with taxonomic, first appearance, last appearance, and geographic data. Genera from the suborder Cimolodonta (boldface), genera from the suborder "Plagiaulacida" (not boldface). J = Jurassic, K = Cretaceous, As = Asia, Au = Australia, Eu = Europe, NA = North America, SA = South America, e = early, m = middle, l = late.

Genus	**Superfamily**	**Family**	**FAD-Epoch**	**FAD-Age**	**FAD-Land Mammal Age**	**FAD-Myr**	**LAD-Epoch**	**LAD-Age**	**LAD-Land Mammal Age**	**LAD-Myr**	**Continent**
Hahnotherium	-	Hahnotheriidae	J Mid	l. Bathon.	-	166	J Mid	l. Bathon.	-	165	Eu
Kermackodon	-	Kermackodontidae	J Mid	l. Bathon.	-	166	J Mid	l. Bathon.	-	165	Eu
Bathmochoffatia	Paulchoffatiid line	Paulchoffatiidae	J Late	e. Kimmer.	-	155	J Late	l. Kimmer.	-	151	Eu
Guimarotodon	Paulchoffatiid line	Paulchoffatiidae	J Late	e. Kimmer.	-	155	J Late	l. Kimmer.	-	151	Eu
Henkelodon	Paulchoffatii	Paulchoffat	J Late	e.	-	155	J Late	l.	-	151	Eu

	d line	iidae		Kimmer.				Kimmer.			
Kielanodon	Paulchoffatii d line	Paulchoffat iidae	J Late	e. Kimmer.	-	155	J Late	l. Kimmer.	-	151	Eu
Meketibolodon	Paulchoffatii d line	Paulchoffat iidae	J Late	e. Kimmer.	-	155	J Late	l. Kimmer.	-	151	Eu
Meketichoffatia	Paulchoffatii d line	Paulchoffat iidae	J Late	e. Kimmer.	-	155	J Late	l. Kimmer.	-	151	Eu
Paulchoffatia	Paulchoffatii d line	Paulchoffat iidae	J Late	e. Kimmer.	-	155	J Late	l. Kimmer.	-	151	Eu
Plesiochoffatia	Paulchoffatii d line	Paulchoffat iidae	J Late	e. Kimmer.	-	155	J Late	l. Kimmer.	-	151	Eu
Proalbionbaatar	Plagiaulacid line	Albionbaat aridae	J Late	e. Kimmer.	-	155	J Late	l. Kimmer.	-	151	Eu
Pseudobolodon	Paulchoffatii d line	Paulchoffat iidae	J Late	e. Kimmer.	-	155	J Late	l. Kimmer.	-	151	Eu
Renatodon	Paulchoffatii d line	Paulchoffat iidae	J Late	e. Kimmer.	-	155	J Late	l. Kimmer.	-	151	Eu
Xenachoffatia	Paulchoffatii	Paulchoffat	J Late	e.	-	155	J Late	l.	-	151	Eu

	d line	iidae		Kimmer.				Kimmer.			
Ctenacodon	Allodontid line	Allodontid ae	J Late	e. Kimmer.	-	155	J Late	e. Tithon.	-	147	NA
Glirodon	Allodontid line	-	J Late	e. Kimmer.	-	155	J Late	e. Tithon.	-	147	NA
Morrisonodon	Allodontid line	Allodontid ae	J Late	e. Kimmer.	-	155	J Late	e. Tithon.	-	147	NA
Psalodon	Allodontid line	Allodontid ae	J Late	e. Kimmer.	-	155	J Late	e. Tithon.	-	147	NA
Zofiabaatar	Allodontid line	Zofiabaatar idae	J Late	e. Kimmer.	-	155	J Late	e. Tithon.	-	147	NA
Kuehneodon	Paulchoffatii d line	Paulchoffat iidae	J Late	e. Kimmer.	-	155	J Late	l. Tithon.	-	146	Eu
Albionbaatar	Plagiaulacid line	Albionbaat aridae	K Early	e. Berrias.	-	146	K Early	l. Berrias.	-	140	Eu
Bernardodon	Paulchoffatii d line	Pinheirodo ntidae	K Early	e. Berrias.	-	146	K Early	l. Berrias.	-	140	Eu
Bolodon	Plagiaulacid	Plagiaulaci	K	e.	-	146	K Early	l. Berrias.	-	140	Eu

	line	dae	Early	Berrias.							
Ecprepaulax	Paulchoffatii d line	Pinheirodo ntidae	K Early	e. Berrias.	-	146	K Early	l. Berrias.	-	140	Eu
Gerhardodon	Paulchoffatii d line	Pinheirodo ntidae	K Early	e. Berrias.	-	146	K Early	l. Berrias.	-	140	Eu
Iberodon	Paulchoffatii d line	Pinheirodo ntidae	K Early	e. Berrias.	-	146	K Early	l. Berrias.	-	140	Eu
Pinheirodon	Paulchoffatii d line	Pinheirodo ntidae	K Early	e. Berrias.	-	146	K Early	l. Berrias.	-	140	Eu
Plagiaulax	Plagiaulacid line	Plagiaulaci dae	K Early	e. Berrias.	-	146	K Early	l. Berrias.	-	140	Eu
Sunnyodon	Paulchoffatii d line	Paulchoffat iidae	K Early	e. Berrias.	-	146	K Early	l. Berrias.	-	140	Eu
Loxaulax	Plagiaulacid line	Eobaatarid ae	K Early	e. Valangin .	-	140	K Early	e. Valangin.	-	139	Eu
Cantalera	Paulchoffatii d line	Pinheirodo ntidae	K Early	l. Hauter.	-	134	K Early	e. Barrem.	-	128	Eu

Lavocatia	Paulchoffatiid line	Pinheirodontidae	K Early	e. Barrem.	-	130	K Early	e. Barrem.	-	128	Eu
Parendotherium	Plagiaulacidline	Eobaataridae	K Early	e. Barrem.	-	130	K Early	e. Barrem.	-	128	Eu
Galveodon	Paulchoffatiid line	Paulchoffatiidae	K Early	e. Barrem.	-	130	K Early	l. Barrem.	-	125	Eu
Hakusanobaatar	Plagiaulacidline	Eobaataridae	K Early	e. Barrem.	-	130	K mid	e. Aptian	-	121	As
Tedoribaatar	Plagiaulacidline	Eobaataridae	K Early	e. Barrem.	-	130	K mid	e. Aptian	-	121	As
Eobaatar	Plagiaulacidline	Eobaataridae	K Early	e. Barrem.	-	130	K mid	l. Albian	-	100	As
Corriebaatar	-	Corriebaataridae	K mid	e. Aptian	-	125	K mid	l. Aptian	-	112	Au
Arginbaatar	-	Arginbaataridae	K mid	e. Aptian	-	125	K mid	l. Albian	-	100	As
Heishanobaatar	Plagiaulacidline	Eobaataridae	K Early	e. Aptian	-	125	K mid	l. Albian	-	100	As

Kielanobaatar	Plagiaulacidline	Albionbaataridae	K Early	e. Aptian	-	125	K mid	l. Albian	-	100	As
Liaobaatar	Plagiaulacidline	Eobaataridae	K mid	e. Aptian	-	125	K mid	l. Albian	-	100	As
Monobaatar	Plagiaulacidline	Eobaataridae	K mid	e. Aptian	-	125	K mid	l. Albian	-	100	As
Sinobaatar	Plagiaulacidline	Eobaataridae	K mid	e. Aptian	-	125	K mid	l. Albian	-	100	As
Ameribaatar	Paracimexomys group	-	K mid	e. Cenoman.	-	100	K mid	e. Cenoman.	-	96	NA
Janumys	Plagiaulacidline	-	K mid	e. Cenoman.	-	100	K mid	e. Cenoman.	-	96	NA
Bryceomys	Paracimexomys group	-	K mid	e. Cenoman.	-	100	K mid	l. Turonian	-	89	NA
Cedaromys	Paracimexom	-	K mid	e.	-	100	K mid	e.	-	74	NA

	ys group			Cenoman.				Cenoman.			
Dakotamys	Paracimexomys group	-	K mid	l. Cenoman.	-	96	K mid	l. Cenoman.	-	94	NA
Cimolodon	Ptilodontoidea	Cimolodontidae	K mid	l. Cenoman.	-	96	K Late	l. Maastrich.	Lancian	66	NA
Uzbekbaatar	-	-	K mid	e. Turon.	-	94	K mid	l. Coniac.	-	86	As
Meniscoessus	-	Cimolomyidae	K Late	e. Santon.	-	86	K Late	l. Maastrich.	Lancian	66	NA
Bulganbaatar	Djadochtatheroidea	-	K Late	e. Campan.	-	84	K Late	e. Campan.	-	81	As
Djadochtatherium	Djadochtatheroidea	Djadochtatheriidae	K Late	e. Campan.	-	84	K Late	e. Campan.	-	81	As
Kamptobaatar	Djadochtatheroidea	Sloanbaataridae	K Late	e. Campan.	-	84	K Late	e. Campan.	-	81	As

Sloanbaatar	Djadochtatheroidea	Sloanbaataridae	K Late	e. Campan.	-	84	K Late	e. Campan.	-	81	As
Tombaatar	Djadochtatheroidea	Djadochtatheriidae	K Late	e. Campan.	-	84	K Late	e. Campan.	-	81	As
Viridomys	-	-	K Late	e. Campan.	Aquilan	84	K Late	e. Campan.	Aquilan	81	NA
Chulsanbaatar	Djadochtatheroidea	-	K Late	e. Campan.	-	84	K Late	l. Campan.	-	71	As
Kryptobaatar	Djadochtatheroidea	Djadochtatheriidae	K Late	e. Campan.	-	84	K Late	l. Campan.	-	71	As
Argentodites	-	-	K Late	e. Campan.	-	84	K Late	l. Maastrich.	-	66	SA
Cimolomys	-	Cimolomyidae	K Late	e. Campan.	Aquilan	84	K Late	l. Maastrich.	Lancian	66	NA
Paracimexomys	Paracimexomys group	-	K mid	l. Santon.	-	84	K Late	l. Maastrich	Lancian	66	NA

								.			
Cimexomys	Paracimexomys group	-	K Late	e. Campan.	Aquilan	84	Paleogene	e. Paleoc.	l. Puercan	64	NA
Mesodma	Ptilodontoidea	Neoplagiaulacidae	K Late	e. Campan.	Aquilan	84	Paleogene	l. Paleoc.	m. Tiffanian	57	NA
Kaiparomys	Ptilodontoidea	Cimolodontidae	K Late	m. Campan.	Judithian	79	K Late	l. Campan.	Judithian	74	NA
Kimbetohia	Ptilodontoidea	Ptilodontidae	K Late	m. Campan.	Judithian	79	Paleogene	e. Paleoc.	l. Puercan	64	NA
Catopsbaatar	Djadochtatheroidea	Djadochtatheriidae	K Late	l. Campan.	-	76	K Late	l. Campan.	-	71	As
Nemegtbaatar	Djadochtatheroidea	-	K Late	l. Campan.	-	76	K Late	l. Campan.	-	71	As
Nessovbaatar	Djadochtatheroidea	Sloanbaataridae	K Late	l. Campan.	-	76	K Late	l. Campan.	-	71	As
Stygimys	-	Eucosmodontidae	K Late	l. Campan.	-	75	Paleogene	e. Paleoc.	l. Torrejo	61	NA

									nian		
Nidimys	Ptilodontoidea	Neoplagiaulacidae	K Late	l. Campan.	"Edmontonian"	74	K Late	e. Maastrich.	"Edmontonian"	69	NA
Barbatodon	-	Kogaionidae	K Late	e. Maastrich.	-	71	K Late	l. Maastrich.	-	66	Eu
Buginbaatar	-	Cimolomyidae	K Late	e. Maastrich.	-	71	K Late	l. Maastrich.	-	66	As
Bubodens	Taeniolabidoidea	Taeniolabididae	K Late	l. Maastrich.	Lancian	69	K Late	l. Maastrich.	Lancian	66	NA
Clemensodon	-	Eucosmodontidae	K Late	l. Maastrich.	Lancian	69	K Late	l. Maastrich.	Lancian	66	NA
Essonodon	-	Cimolomyidae	K Late	l. Maastric	Lancian	69	K Late	l. Maastrich	Lancian	66	NA

				h.				.			
Kogaionon	-	Kogaionidae	K Late	l. Maastrich.	-	69	K Late	l. Maastrich.	-	66	Eu
Paressonodon	-	Cimolomyidae	K Late	l. Maastrich.	Lancian	69	K Late	l. Maastrich.	Lancian	66	NA
Parikimys	Ptilodontoidea	Neoplagiaulacidae	K Late	l. Maastrich.	Lancian	69	K Late	l. Maastrich.	Lancian	66	NA
Hainina	-	Kogaionidae	K Late	l. Maastrich.	-	69	Paleogene	l. Paleoc.	Thanetian	55	Eu
Neoplagiaulax	Ptilodontoidea	Neoplagiaulacidae	K Late	l. Maastrich.	Lancian	69	Paleogene	l. Paleoc.	Thanetian	55	NA
Parectypodus	Ptilodontoidea	Neoplagiaulacidae	K Late	l. Maastric	Lancian	69	Paleogene	e. Eocene	l. Wasatc	52	NA

				h.					hian		
Xyronomys	Ptilodontoidea	Neoplagiaulacidae	Paleogene	e. Paleoc.	e. Puercan	66	Paleogene	e. Paleoc.	m. Torrejonian	61	NA
Acheronodon	-	Microcosmodontidae	Paleogene	e. Paleoc.	e. Puercan	66	Paleogene	l. Paleoc.	e. Tiffanian	60	NA
Catopsalis	Taeniolabidoidea	Taeniolabididae	Paleogene	e. Paleoc.	e. Puercan	66	Paleogene	l. Paleoc.	m. Tiffanian	57	NA
Ptilodus	Ptilodontoidea	Ptilodontidae	Paleogene	e. Paleoc.	e. Puercan	66	Paleogene	l. Paleoc.	l. Tiffanian	56	NA
Ectypodus	Ptilodontoidea	Neoplagiaulacidae	Paleogene	e. Paleoc.	e. Puercan	66	Paleogene	l. Eocene	m. Chadronian	35	NA
Taeniolabis	Taeniolabidoidea	Taeniolabididae	Paleogene	e. Paleoc.	m. Puercan	65	Paleogene	e. Paleoc.	l. Puercan	64	NA

Eucosmodon	-	Eucosmodontidae	Paleogene	e. Paleoc.	m. Puercan	65	Paleogene	e. Paleoc.	l. Torrejonian	61	NA
Cernaysia	Ptilodontoidea	Neoplagiaulacidae	Paleogene	l. Paleoc.	-	65	Paleogene	l. Paleoc.	-	56	Eu, NA
Microcosmodon	-	Microcosmodontidae	Paleogene	e. Paleoc.	m. Puercan	65	Paleogene	l. Paleoc.	l. Clarkforkian	55	NA
Xanclomys	Ptilodontoidea	Neoplagiaulacidae	Paleogene	e. Paleoc.	m. Torrejonian	62	Paleogene	e. Paleoc.	m. Torrejonian	61	NA
Krauseia	Ptilodontoidea	Neoplagiaulacidae	Paleogene	e. Paleoc.	m. Torrejonian	62	Paleogene	l. Paleoc.	e. Tiffanian	60	NA
Anconodon	Ptilodontoidea	Cimolodontidae	Paleogene	e. Paleoc.	m. Torrejonian	62	Paleogene	l. Paleoc.	e. Tiffanian	59	NA
Boffius	-	Boffiidae	Paleog	m.	-	62	Paleogene	m.	-	59	Eu

			ene	Paleoc.				Paleoc.			
Baiotomeus	Ptilodontoidea	Ptilodontidae	Paleogene	e. Paleoc.	l. Torrejonian	62	Paleogene	l. Paleoc.	m. Tiffanian	58	NA
Mimetodon	Ptilodontoidea	Neoplagiaulacidae	Paleogene	e. Paleoc.	l. Torrejonian	62	Paleogene	l. Paleoc.	l. Tiffanian	56	NA
Fractinus	-	-	Paleogene	l. Paleoc.	e. Tiffanian	61	Paleogene	l. Paleoc.	e. Tiffanian	60	NA
Allocosmodon	-	Microcosmodontidae	Paleogene	l. Paleoc.	e. Tiffanian	61	Paleogene	l. Paleoc.	m. Tiffanian	57	NA
Pentacosmodon	-	Microcosmodontidae	Paleogene	l. Paleoc.	e. Tiffanian	61	Paleogene	l. Paleoc.	l. Tiffanian	56	NA
Liotomus	Ptilodontoidea	Cimolodontidae	Paleogene	l. Paleoc.	e. Tiffanian	61	Paleogene	l. Paleoc.	Thanetian	55	NA/Eu

Lambdopsalis	Taeniolabidoidea	Taeniolabididae	Paleogene	l. Paleoc.	-	59	Paleogene	l. Paleoc.	-	55	As
Prionessus	Taeniolabidoidea	Taeniolabididae	Paleogene	l. Paleoc.	-	59	Paleogene	l. Paleoc.	-	55	As
Prochetodon	Ptilodontoidea	Ptilodontidae	Paleogene	l. Paleoc.	l. Tiffanian	59	Paleogene	l. Paleoc.	l. Clarkforkian	55	NA
Sphenopsalis	Taeniolabidoidea	Taeniolabididae	Paleogene	l. Paleoc.	-	59	Paleogene	l. Paleoc.	-	55	As
Neoliotomus	Ptilodontoidea	-	Paleogene	l. Paleoc.	l. Tiffanian	57	Paleogene	e. Eocene	m. Wasatchian	53	NA
Mesodmops	Ptilodontoidea	Neoplagiaulacidae	Paleogene	l. Paleoc.	-	56	Paleogene	e. Eocene	-	50	As

Supplementary Table 4. Generic richness data from Supplementary Table 3 partitioned into 5-Myr bins.

Bin start age (Myr)	Bin end age (Myr)	Bin midpoint (Myr)	# of genera
171	166	168.5	0
166	161	163.5	2
161	156	158.5	0
156	151	153.5	12
151	146	148.5	6
146	141	143.5	9
141	136	138.5	10
136	131	133.5	1
131	126	128.5	7
126	121	123.5	11
121	116	118.5	8
116	111	113.5	8
111	106	108.5	7
106	101	103.5	7
101	96	98.5	11
96	91	93.5	5

Bin start age (Myr)	Bin end age (Myr)	Bin midpoint (Myr)	# of genera
91	86	88.5	4
86	81	83.5	16
81	76	78.5	12
76	71	73.5	17
71	66	68.5	21
66	61	63.5	22
61	56	58.5	25
56	51	53.5	11
51	46	48.5	2
46	41	43.5	1
41	36	38.5	1
36	31	33.5	1

Supplementary Table 5. Body mass estimates of multituberculate species. Length and width measurements for lower first molar area (m1 area), skull length measurements (SL), and temporal range data (First Appearance Datum [FAD], Last Appearance Datum [LAD]) were compiled from cited sources. The SL formula is from ref. 39. For species without skull length data, m1 area estimates (ref. 35) were used to predict SL estimates based on a regression analysis (m1-SL; this study).

Species	**FAD (Myr)**	**LAD (Myr)**	**m1 area (mm^2)**	**SL (mm)**	**Body mass (kg)**	**Predictive formula**	**Data sources**
Acheronodon vossae	61	60	2.43	-	0.036	m1-SL	[53]
Allocosmodon woodi	61	57	2.88	-	0.046	m1-SL	[53]
Anconodon cochranensis	61	60	3.34	-	0.057	m1-SL	[54]
Arginbaatar dmitrievae	125	100	1.35	-	0.011	m1-SL	[55]
Baiotomeus douglassi	62	61	6.65	-	0.154	m1-SL	[56]
Baiotomeus rhothonion	62	61	1.62	-	0.020	m1-SL	[57]
Barbatodon transylvanicus	71	66	7.37	-	0.178	m1-SL	[58]
Boffius splendidus	62	59	134.69	-	11.808	m1-SL	[59]
Bolodon minor	146	140	0.96	-	0.006	m1-SL	[60,61]

Bolodon osborni	146	140	1.74	-	0.022	m1-SL	[62]
Bryceomys fumosus	94	89	1.46	-	0.017	m1-SL	[63]
Bryceomys hadrosus	94	89	4.28	-	0.081	m1-SL	[63]
Bryceomys intermedius	100	96	2.16	-	0.030	m1-SL	[64]
Bubodens magnus	69	66	76.80	-	5.248	m1-SL	[65]
Catopsalis alexanderi	66	65	41.92	-	2.190	m1-SL	[66]
Catopsalis calgariensis	61	60	139.73	-	12.451	m1-SL	[66]
Catopsalis fissidens	64	61	82.41	-	5.811	m1-SL	[67,68]
Catopsalis foliatus	66	64	52.43	-	3.025	m1-SL	[68]
Catopsalis joyneri	66	65	45.11	-	2.435	m1-SL	[69]
Catopsalis waddleae	65	64	152.52	-	14.128	m1-SL	[70]
Catopsbaatar catopsaloides	76	71	19.36	63.00	0.879	SL	[71,72]
Cedaromys bestia	100	96	3.91	-	0.071	m1-SL	[64]
Cedaromys hutchisoni	79	74	2.29	-	0.033	m1-SL	[73]
Cedaromys parvus	100	96	2.86	-	0.046	m1-SL	[64]

cf. *Paracimexomys perplexus*	100	96	1.58	-	0.019	m1-SL	[64]
cf. *Paracimexomys robisoni*	100	96	1.92	-	0.026	m1-SL	[63]
Chulsanbaatar vulgaris	84	71	1.53	18.50	0.012	SL	[71]
Cimexomys antiquus	84	79	2.37	-	0.035	m1-SL	[74]
Cimexomys arapahoensis	66	65	5.09	-	0.104	m1-SL	[75]
Cimexomys gratus	66	64	5.35	-	0.112	m1-SL	[76]
Cimexomys judithae	79	74	1.97	-	0.027	m1-SL	[77]
Cimexomys minor	69	64	3.10	-	0.051	m1-SL	[78]
Cimolodon electus	84	74	6.63	-	0.153	m1-SL	[74]
Cimolodon foxi	86	74	2.87	-	0.046	m1-SL	[79]
Cimolodon nitidus	86	66	7.40	-	0.179	m1-SL	[78,80,81]
Cimolodon similis	94	81	5.10	-	0.105	m1-SL	[74,82]
Cimolodon wardi	84	81	3.87	-	0.070	m1-SL	[82]
Cimolomys butleria	79	74	4.05	-	0.075	m1-SL	[73]
Cimolomys clarki	79	74	8.43	-	0.216	m1-SL	[83]

Cimolomys gracilis	74	66	10.26	-	0.287	m1-SL	[78,84]
Ctenacodon scindens	155	147	1.58	-	0.019	m1-SL	[85,86]
Ctenacodon serratus	155	147	1.31	-	0.010	m1-SL	[86-88]
Dakotamys malcolmi	96	94	2.14	-	0.030	m1-SL	[63]
Djadochtatherium matthewi	84	81	10.84	-	0.311	m1-SL	[89,90]
Ectypodus aphronorus	62	60	1.52	-	0.018	m1-SL	[54,91]
Ectypodus childei	55	49	1.88	-	0.025	m1-SL	[92]
Ectypodus elaphus	59	58	1.32	-	0.010	m1-SL	[93]
Ectypodus lovei	43	35	1.56	-	0.019	m1-SL	[94,95]
Ectypodus musculus	61	56	2.50	-	0.037	m1-SL	[96]
Ectypodus powelli	61	55	1.90	-	0.025	m1-SL	[97]
Ectypodus szalayi	62	60	1.76	-	0.022	m1-SL	[92]
Ectypodus tardus	59	53	1.45	-	0.012	m1-SL	[98]
Eobaatar clemensi	130	125	1.50	-	0.018	m1-SL	[99]
Eobaatar magnus	125	100	1.87	-	0.025	m1-SL	[55]

Essonodon browni	69	66	29.96	-	1.349	m1-SL	[76]
Eucosmodon americanus	65	64	14.56	-	0.476	m1-SL	[96]
Glirodon grandis	155	147	2.21	-	0.031	m1-SL	[100]
Guimarotodon leiriensis	155	151	2.85	-	0.045	m1-SL	[101]
Hainina belgica	66	61	1.63	-	0.020	m1-SL	[59]
Hainina godfriauxi	66	55	5.18	-	0.107	m1-SL	[59]
Hainina pyrenaica	66	65	3.05	-	0.050	m1-SL	[102]
Hainina vianeyae	61	55	4.06	-	0.075	m1-SL	[102,103]
Heishanobaatar triangulus	125	100	1.86	-	0.024	m1-SL	[104]
Iberodon quadrituberculatus	146	140	1.73	-	0.022	m1-SL	[105]
Janumys erebos	100	96	0.96	-	0.006	m1-SL	[64]
Kaiparomys cifellii	79	74	4.50	-	0.087	m1-SL	[73]
Kamptobaatar kuczynskii	84	81	1.98	19.00	0.013	SL	[106]
Kimbetohia mziae	66	65	3.92	-	0.072	m1-SL	[75]
Krauseia clemensi	62	60	2.20	-	0.031	m1-SL	[92,103]

Kryptobaatar dashzevegi	84	71	3.41	32.00	0.083	SL	[106]
Kryptobaatar mandahuensis	84	71	3.52	-	0.061	m1-SL	[107]
Kuehneodon dietrichi	155	151	2.64	-	0.040	m1-SL	[108]
Kuehneodon uniradiculatus	155	151	2.72	-	0.042	m1-SL	[108]
Lambdopsalis bulla	59	56	28.00	60.78	0.776	SL	[109]
Liaobaatar changi	125	100	4.89	-	0.099	m1-SL	[110]
Liotomus marshi	61	55	7.13	-	0.170	m1-SL	[103]
Loxaulax valdensis	140	139	3.20	-	0.053	m1-SL	[55,61,111]
Meketibolodon robustus	155	151	2.97	-	0.048	m1-SL	[101]
Meniscoessus collomensis	74	66	19.84	-	0.744	m1-SL	[112]
Meniscoessus intermedius	86	69	11.13	-	0.323	m1-SL	[113]
Meniscoessus major	79	69	15.39	-	0.516	m1-SL	[113]
Meniscoessus robustus	74	66	31.92	69.00	1.208	SL	[86]
Meniscoessus seminoensis	69	66	32.21	-	1.497	m1-SL	[114]
Mesodma ambigua	66	64	3.38	-	0.058	m1-SL	[96]

Mesodma archibaldi	79	74	1.61	-	0.020	m1-SL	[73]
Mesodma formosa	69	64	2.37	-	0.035	m1-SL	[78,80,84,115]
Mesodma garfieldensis	66	65	2.73	-	0.042	m1-SL	[76]
Mesodma hensleighi	69	64	1.48	-	0.018	m1-SL	[80,84,115]
Mesodma minor	79	74	1.26	-	0.009	m1-SL	[73,79,82]
Mesodma primaeva	79	74	6.00	-	0.132	m1-SL	[116]
Mesodma pygmaea	62	57	1.02	-	0.006	m1-SL	[91]
Mesodma senecta	84	79	3.20	-	0.053	m1-SL	[117]
Mesodma thompsoni	74	64	3.19	-	0.053	m1-SL	[80,81,84,115]
Mesodmops dawsonae	55	50	2.59	-	0.039	m1-SL	[118]
Mesodmops tenuis	56	55	1.98	-	0.027	m1-SL	[119]
Microcosmodon arcuatus	64	64	2.48	-	0.037	m1-SL	[120]
Microcosmodon conus	59	56	2.78	-	0.044	m1-SL	[53]
Microcosmodon harleyi	65	64	2.01	-	0.027	m1-SL	[121]
Microcosmodon rosei	56	55	2.31	-	0.033	m1-SL	[97]

Mimetodon churchilli	57	56	4.48	-	0.087	m1-SL	[96]
Mimetodon silberlingi	62	57	2.08	-	0.029	m1-SL	[122]
Nemegtbaatar gobiensis	76	71	4.42	42.00	0.214	SL	[71]
Neoliotomus conventus	57	55	23.10	-	0.527	m1-SL	[97]
Neoliotomus ultimus	56	53	23.00	-	0.921	m1-SL	[13]
Neoplagiaulax annae	61	55	3.07	-	0.050	m1-SL	[103]
Neoplagiaulax cimolodontoides	59	58	2.46	-	0.037	m1-SL	[93]
Neoplagiaulax copei	61	55	4.62	-	0.091	m1-SL	[103]
Neoplagiaulax donaldorum	61	59	3.12	-	0.052	m1-SL	[123]
Neoplagiaulax eocaenus	61	55	1.77	-	0.023	m1-SL	[103]
Neoplagiaulax grangeri	62	60	4.71	-	0.093	m1-SL	[54]
Neoplagiaulax hazeni	59	56	4.48	-	0.087	m1-SL	[96]
Neoplagiaulax hunteri	62	57	2.98	-	0.048	m1-SL	[57,122]
Neoplagiaulax macrotomeus	62	61	1.62	-	0.020	m1-SL	[124]
Neoplagiaulax mckennai	59	57	3.51	-	0.061	m1-SL	[91]

Neoplagiaulax nicolai	61	55	5.49	-	0.117	m1-SL	[103]
Neoplagiaulax paskapooensis	59	58	2.98	-	0.048	m1-SL	[93]
Neoplagiaulax serrator	59	58	2.44	-	0.036	m1-SL	[93]
Nessovbaatar multicostatus	76	71	2.00	-	0.027	m1-SL	[90]
Nidimys occultus	74	69	5.14	-	0.106	m1-SL	[125]
Paracimexomys magister	84	81	4.48	-	0.087	m1-SL	[74]
Paracimexomys priscus	69	66	3.85	-	0.070	m1-SL	[80,81]
Paracimexomys propriscus	79	69	2.90	-	0.046	m1-SL	[125]
Parectypodus clemensi	62	61	2.93	-	0.047	m1-SL	[126]
Parectypodus corystes	62	61	2.97	-	0.048	m1-SL	[57]
Parectypodus foxi	69	66	4.17	-	0.078	m1-SL	[115]
Parectypodus laytoni	58	55	1.36	-	0.011	m1-SL	[97]
Parectypodus lunatus	55	52	2.03	-	0.028	m1-SL	[98]
Parectypodus simpsoni	55	53	2.70	-	0.042	m1-SL	[98]
Parectypodus sinclairi	62	58	1.57	-	0.019	m1-SL	[54]

Parectypodus sylviae	62	60	1.73	-	0.022	m1-SL	[126]
Parectypodus trovessartianus	62	61	4.65	-	0.092	m1-SL	[96]
Parikimys carpenteri	69	66	2.89	-	0.046	m1-SL	[127]
Pentacosmodon pronus	58	56	3.28	-	0.055	m1-SL	[53,96]
Pinheirodon pygmaeus	146	140	1.23	-	0.009	m1-SL	[105]
Pinheirodon vastus	146	140	2.07	-	0.028	m1-SL	[105]
Plagiaulax becklesii	146	140	2.47	-	0.037	m1-SL	[60,61]
Prionessus lucifer	59	56	12.20	-	0.369	m1-SL	[128]
Prochetodon cavus	58	56	5.43	-	0.115	m1-SL	[129]
Prochetodon foxi	59	57	6.83	-	0.160	m1-SL	[129]
Prochetodon taxus	56	55	6.55	-	0.150	m1-SL	[129]
Psalodon marshi	155	147	3.42	-	0.059	m1-SL	[85,86]
Ptilodus fractus	59	56	5.12	-	0.105	m1-SL	[130]
Ptilodus gnomus	62	59	3.77	-	0.068	m1-SL	[57,131]
Ptilodus kummae	59	57	5.28	-	0.110	m1-SL	[122]

Ptilodus mediaevus	64	56	6.93	-	0.163	m1-SL	[126,132]
Ptilodus montanus	62	57	5.98	38.97	0.165	SL	[54,132]
Ptilodus wyomingensis	62	57	6.44	-	0.147	m1-SL	[96]
Sinobaatar fuxinensis	125	100	2.71	-	0.042	m1-SL	[110]
Sinobaatar xiei	125	100	2.40	-	0.035	m1-SL	[110]
Sloanbaatar mirabilis	84	81	1.70	22.30	0.023	SL	[106]
Stygimys jepseni	62	61	4.37	-	0.084	m1-SL	[54]
Stygimys kuszmauli	66	64	8.30	-	0.212	m1-SL	[76]
Taeniolabis lamberti	65	64	128.00	-	10.971	m1-SL	[133]
Taeniolabis taoensis	64	64	205.92	160.00	22.697	SL	[133]
Uzbekbaatar wardi	91	86	2.20	-	0.031	m1-SL	[134]
Xyronomys robinsoni	66	65	1.87	-	0.025	m1-SL	[75]

Supplementary Table 6. OPC and OPCR results for carnivorans and rodents in Evans et al.[18].

Species	OPC (l)	OPCR (l)	OPC (u)	OPCR (u)
Acinonyx jubatus	40	36.5	53	52.625
Ailuropoda melanoleuca	257	266.625	342	326.25
Ailurus fulgens	195	194.625	270	269.875
Alopex lagopus	95	96.75	174	154.25
Canis aureus	125	132.875	185	172.625
Canis lupus	97	97.375	137	135.25
Crocuta crocuta	61	55.875	72	76.125
Felis silvestris	37	44.625	55	62.25
Galerella sanguinea	110	107.125	143	144.25
Genetta genetta	140	139.5	144	143.875
Gulo gulo	54	54.25	124	122.5
Herpestes ichneumon	101	101.125	149	144.25
Lutra lutra	91	89.875	150	152.875
Lynx lynx	40	44.75	58	62.25
Martes foina	79	72.5	145	143.75
Martes martes	77	79.875	142	138.125
Meles meles	121	118.875	195	194.625
Mustela erminea	39	43.5	76	76.875
Mustela eversmannii	48	46.75	91	83.5
Mustela lutreola	68	71.25	126	119.25
Mustela nivalis	54	54.5	90	89.875
Mustela putorius	55	55.875	99	99.625
Otocyon megalotis	162	163.625	184	176.5
Panthera leo	37	41.125	53	57.375
Paradoxurus leucomystax	115	121.75	115	114.25

Procyon lotor	153	154.75	188	180.375
Ursus americanus	192	194.125	150	164.5
Ursus arctos	179	185.625	170	172.5
Ursus maritimus	201	189.75	135	137.875
Viverra zibetha	162	161.375	206	203
Vormela peregusna	56	56.75	113	113.25
Vulpes vulpes	119	117.625	184	173.25
Aethomys hindei	225	222.25	231	241.625
Akodon serrensis	113	114.75	129	128
Anisomys imitator	231	235.125	280	280.875
Apodemus agrarius	173	176.375	173	176.125
Arvicanthis niloticus	150	153.625	182	185.875
Berylmys bowersi	193	187.875	209	204.125
Crateromys schadenbergi	230	233.375	285	283.75
Dasymys sp.	233	233.875	309	305.25
Geoxus valdivianus	184	175.625	191	184.5
Grammomys dolichurus	229	228.5	265	265
Grammomys rutilans	220	238.25	273	282.625
Holochilus brasiliensis	287	281.75	285	275.875
Hybomys univittatus	220	215.5	233	234.625
Hydromys chrysogaster	122	122.125	126	133.125
Hylomyscus stella	190	189.375	177	180.25
Hyomys goliath	277	269.375	309	303.625
Ichthyomys stolzmanni	163	159.875	182	184.125
Lemniscomys striatus	167	166.75	218	222.625
Leopoldamys sabanus	217	227.875	229	232.25
Leptomys elegans	149	147.875	134	132.375
Lophuromys medicaudatus	167	165.25	256	259.875
Malacomys sp.	180	187.25	206	207.625
Mallomys rothschildi	241	241.5	259	259.375

Mastomys natalensis	152	155.375	167	179.875
Melomys levipes	177	182.375	189	196
Micromys minutus	164	166.5	162	164.75
Mus musculus	167	173.375	181	176.625
Nectomys squamipes	226	220.625	253	260.875
Nesokia indica	191	189.125	237	236.125
Notomys mitchellii	181	180.125	203	206.25
Oenomys hypoxanthus	187	198.25	190	192.375
Otomys denti	146	140	197	189.375
Otomys irroratus	133	128.75	167	172.75
Oxymycterus sp.	153	158.875	130	140
Parotomys littledalei	173	176.75	212	222.75
Pelomys campanae	189	191.875	196	202.5
Peromyscus maniculatus	200	190.5	201	204.875
Phyllotis sp	214	215.875	181	183.875
Pogonomys sp	246	247.5	293	279.75
Praomys jacksoni	177	178.375	162	162.25
Rattus leucopus	239	246.125	236	236.75
Reithrodon auritus	222	232	247	250.5
Reithrodontomys mexicanus	256	252.25	276	257.5
Rhabdomys pumilio	180	177.625	185	188.25
Sigmodon hispidus	267	258	276	293.875
Stochomys longicaudatus	265	269	266	267.25
Sundamys muelleri	203	212.625	245	232.625
Uromys caudimaculatus	184	202.75	197	207
Zygodontomys sp.	178	175.625	202	189.625

Supplementary Table 7. Comparisons of OPC results for two multituberculate tooth row casts (*Meniscoessus robustus* UCMP 107405, *Parikimys carpenteri* DMNH 52224) for three 3D scanners. Relative standard errors for the two casts were 0.98% and 3.06% respectively.

Species	**Scanner**	**OPCR**
M. robustus	MicroCT	168.375
M. robustus	Hawk	164.25
M. robustus	Laser Design	163
P. carpenteri	MicroCT	144.875
P. carpenteri	Hawk	134.875
P. carpenteri	Laser Design	130.75

References

30. Evans, A. R. Connecting morphology, function and tooth wear in microchiropterans. *Biological Journal of the Linnean Society* **85**, 81-96 (2005).

31. Evans, A. R., Fortelius, M. & Jernvall, J. How does tooth wear affect dental complexity? Implications for tooth function and dietary reconstruction. *Journal of Vertebrate Paleontology* **27**, 72A (2007).

32. Woodburne, M. O. 400 (Columbia University Press, New York, 2004).

33. Gradstein, F. in *A Geologic Time Scale 2004* (eds Felix Gradstein, James Ogg, & Alan Smith) 1-46 (Cambridge University Press, 2004).

34. Damuth, J. & MacFadden, B. J. 397 (Cambridge University Press, Cambridge, 1990).

35. Legendre, S. Analysis of mammalian communities from the Late Eocene and Oligocene of southern France. *Palaeovertebrata* **16**, 191-212 (1986).

36. McDermott, B., Hunter, J. & Alroy, J. Estimating body mass of multituberculate mammals. *Journal of Vertebrate Paleontology* **22**, 86A (2002).

37. Hopkins, S. S. B. Reassessing the mass of exceptionally large rodents using toothrow length and area as proxies for body mass. *Journal of Mammalogy* **89**, 232-243 (2008).

38. Millien, V. The largest among the smallest: The body mass of the giant rodent *Josephoartigasia monesi*. *Proceedings of the Royal Society B* **275**, 1953-1955 (2008).

39. Millien, V. & Bovy, H. When teeth and bones disagree: Body mass estimation of a giant extinct rodent. *Journal of Mammalogy* **91**, 11-18 (2010).

40. Janis, C. M. in *Body Size in Mammalian Paleobiology: Estimation and Biological Implications* (eds John Damuth & Bruce J. MacFadden) 255-299 (Cambridge University Press, 1990).

41. Luo, Z.-X., Crompton, A. W. & Sun, A.-L. A new mammaliaform from the Early Jurassic and evolution of mammalian characteristics. *Science* **292**, 1535-1540 (2001).

42. Foster, J. R. Preliminary body mass estimates for mammalian genera of the Morrison Formation (Upper Jurassic, North America). *PaleoBios* **28**, 114-122 (2009).

43. Kleiber, M. Body size and metabolic rate. *Physiological Reviews* **27**, 511-541 (1947).

44. Kleiber, M. Metabolic turnover rate: A physiological meaning of the metabolic rate per unit body weight. *Journal of Theoretical Biology* **53**, 199-204 (1975).

45. McNab, B. K. in *Body size in mammalian paleobiology: Estimation and biological implications* (eds John Damuth & Bruce J. MacFadden) 11-24 (Cambridge University Press, 1990).

46. Peters, R. H. *The ecological implications of body size*. (Cambridge University Press, 1983).

47. Schimdt-Nielsen, K. *Scaling: Why is animal size so important?* , (Cambridge University Press, 1984).

48. Demment, M. W. & Van Soest, P. J. A nutritional explanation for body-size patterns of ruminant and nonruminant herbivores. *The American Naturalist* **125**, 641-672 (1985).

49. Lucas, P. W. *Dental Functional Morphology: How Teeth Work*. (Cambridge University Press, 2004).

50. Van Soest, P. J. Allometry and ecology of feeding behavior and digestive capacity in herbivores: A review. *Zoo Biology* **15**, 455-479 (1996).

51. Manly, B. F. J. *Randomization, Bootstrap and Monte Carlo Methods in Biology*. 3rd edn, 399 (Chapman and Hall/CRC, 2006).

52. R: A language and environment for statistical computing (R Foundation for Statistical Computing, Vienna, Austria, 2011).

53. Fox, R. C. Microcosmodontid multituberculates (Allotheria, Mammalia) from the Paleocene and Late Cretaceous of western Canada. *Palaeontographica Canadiana* **23**, 1-109 (2005).

54. Simpson, G. G. The Fort Union of the Crazy Mountain Field, Montana and its mammalian faunas. *Bulletin of the United States National Museum* **169**, 1-287 (1937).

55. Kielan-Jaworowska, Z., Dashzeveg, D. & Trofimov, B. A. Early Cretaceous multituberculates from Mongolia and a comparison with Late Jurassic forms. *Acta Palaeontologica Polonica* **32**, 3-47 (1987).

56. Krause, D. W. *Baiotomeus*, a new ptilodontoid multituberculate (Mammalia) from the middle Paleocene of Western North America. *Journal of Paleontology* **61**, 595-603 (1987).

57. Scott, C. S. Late Torrejonian (Middle Paleocene) mammals from south central Alberta, Canada. *Journal of Paleontology* **77**, 745-768 (2003).

58. Csiki, Z., Grigorescu, D. & Rücklin, M. A new multituberculate specimen from the Maastrichtian of Pui, Romania and reassessment of affinities of *Barbatodon*. *Acta Palaeontologica Romaniae* **5**, 73-86 (2005).

59. Vianey-Liaud, M. Les Mammiferes Montiens de Hainin (Paleocene Moyen de Belgique) Part I: Multitubercules. *Palaeovertebrata* **9**, 117-131 (1979).

60. Falconer, H. Description of two species of fossil mammalian genus *Plagiaulax* from Purbeck. *Quarterly Journal of the Geological Society of London* **13**, 261-282 (1857).

61. Simpson, G. G. *A Catalogue of the Mesozoic Mammalia in the Geological Department of the British Museum*. (Trustees of the British Museum, 1928).

62. Kielan-Jaworowska, Z. & Enson, P. C. Multituberculate mammals from the Upper Jurassic Purbeck Limestone Formation of southern England. *Palaeontology* **35**, 95-126 (1992).

63. Eaton, J. G. Cenomanian and Turonian (early Late Cretaceous) multituberculate mammals from southwestern Utah. *Journal of Vertebrate Paleontology* **15**, 761-784 (1995).

64. Eaton, J. G. & Cifelli, R. L. Multituberculate mammals from near the Early-Late Cretaceous boundary, Cedar Mountain Formation, Utah. *Acta Palaeontologica Polonica* **46**, 453-518 (2001).

65. Wilson, R. W. Late Cretaceous (Fox Hills) multituberculates from the Red Owl local fauna of western North Dakota. *Dakoterra* **3**, 118-132 (1987).

66. Middleton, M. D. A new species and additional material of *Catopsalis* (Mammalia: Multituberculata) from the Western Interior of North America. *Journal of Paleontology* **56**, 1197-11206 (1982).

67. Lucas, S. G., Williamson, T. E. & Middleton, M. D. *Catopsalis* (Mammalia: Multituberculata) from the Paleocene of New Mexico and Utah: Taxonomy and biochronological significance. *Journal of Paleontology* **71**, 484-493 (1997).

68. Granger, W. & Simpson, G. G. A revision of the Tertiary Multituberculata. *Bulletin of the American Museum of Natural History* **56**, 601-676 (1929).

69. Kielan-Jaworowska, Z. & Sloan, R. E. *Catopsalis* (Multituberculata) from Asia and North America and the problem of Taeniolabidid dispersal in the Late Cretaceous. *Acta Palaeontologica Polonica* **24**, 187-197 (1979).

70. Buckley, G. The multituberculate *Catopsalis* from the early Paleocene of the Crazy Mountains Basin in Montana. *Acta Palaeontologica Polonica* **40**, 389-398 (1995).

71. Kielan-Jaworowska, Z. Multituberculate succession in the Late Cretaceous of the Gobi Desert (Mongolia). *Acta Palaeontologica Polonica* **30** (1974).

72. Kielan-Jaworowska, Z., Hurum, J. & Lopatin, A. V. Skull structure in *Catopsbaatar* and the zygomatic ridges in multituberculate mammals. *Acta Palaeontologica Polonica* **50**, 487-512 (2005).

73. Eaton, J. G. Multituberculate mammals from the Wahweap (Campanian, Aquilan) and Kaiparowits (Campanian, Judithian) formations, within and near Grand Staircase-Escalante National Monument, southern Utah. *Miscellaneous Publications of the Utah Geological Survey* **4**, 1-66 (2002).

74. Fox, R. C. Early Campanian multituberculates (Mammalia: Allotheria) from the upper Milk River Formation, Alberta. *Canadian Journal of Earth Sciences* **8**, 916-938 (1971).

75. Middleton, M. D. & Dewar, E. W. in *Paleogene Mammals* Vol. 26 (eds S.G. Lucas, K.E. Zeigler, & P.E. Kondrashov) 59-80 (New Mexico Museum of Natural History and Science Bulletin, 2004).

76. Archibald, J. D. A study of Mammalia and geology across the Cretaceous-Tertiary boundary in Garfield County, Montana. *University of California Publications in Geological Sciences* **122**, 1-286 (1982).

77. Montellano, M., Weil, A. & Clemens, W. A. An exceptional specimen of *Cimexomys judithae* (Mammalia: Multituberculata) from the Campanian Two Medicine Formation of Montana, and the phylogenetic status of *Cimexomys*. *Journal of Vertebrate Paleontology* **20**, 333-340 (2000).

78. Clemens, W. A. Fossil mammals of the type Lance Formation, Wyoming: Part I. Introduction and Multituberculata. *University of California Publications in Geological Sciences* **48**, 1-105 (1964).

79. Eaton, J. G. Santonian (Late Cretaceous) mammals from the John Henry Member of the Straight Cliffs Formation, Grand Staircase-Escalante National Monument, Utah. *Journal of Vertebrate Paleontology* **26**, 446-460 (2006).

80. Lillegraven, J. A. Latest Cretaceous mammals of upper part of Edmonton Formation of Alberta, Canada, and review of marsupial-placental dichotomy in mammalian evolution. *The University of Kansas Paleontological Contributions* **50**, 1-122 (1969).

81. Fox, R. C. The Wounded Knee local fauna and mammalian evolution near the Cretaceous-Tertiary boundary, Saskatchewan, Canada. *Palaeontographica Abt. A* **208**, 11-59 (1989).

82. Eaton, J. G. in *Late Cretaceous vertebrates from the Western Interior* Vol. 35 (eds Spencer G. Lucas & Robert M. Sullivan) 373-402 (New Mexico Museum of Natural History and Science Bulletin, 2006).

83. Lillegraven, J. A. & McKenna, M. C. Fossil mammals from the "Mesaverde" Formation (Late Cretaceous, Judithian) of the Bighorn and Wind River basins, Wyoming, with definitions of Late Cretaceous North American land-mammal "ages". *American Museum Novitates* **2840**, 1-68 (1986).

84. Webb, M. W. *Fluvial architecture and Late Cretaceous mammals of the Lance Formation, southwestern Bighorn Basin, Wyoming*, University of Wyoming, (2001).

85. Simpson, G. G. American Mesozoic Mammalia. *Memoirs of the Peabody Museum of Yale University* **3**, 1-235 (1929).

86. GPW measurement.

87. Marsh, O. C. Notice of new Jurassic mammals. *American Journal of Science* **18**, 396-398 (1879).

88. Carpenter, K. Redescription of the multituberculate, *Zofiabaatar* and the paurodont, *Foxraptor*, from the Pine Tree Ridge, Wyoming. *Modern Geology* **23**, 393-405 (1998).

89. Simpson, G. G. A Mesozoic mammal skull from Mongolia. *American Museum Novitates* **201**, 1-11 (1925).

90. Kielan-Jaworowska, Z. & Hurum, J. Djadochtatheria - a new suborder of multituberculate mammals. *Acta Palaeontologica Polonica* **42**, 201-242 (1997).

91. Sloan, R. E. in *The Cretaceous-Tertiary boundary in the San Juan and Raton Basins, New Mexico and Colorado* Vol. 209 (eds James E. Fassett & J. Keith Rigby, Jr.) 165-200 (Geological Society of America Special Paper, 1987).

92. Sloan, R. E. in *Advances in San Juan Basin Paleontology* (eds Spencer G. Lucas, J. Keith Rigby, Jr., & Barry Kues) 127-160 (University of New Mexico Press, 1981).

93. Scott, C. S. New neoplagiaulacid multituberculates (Mammalia: Allotheria) from the Paleocene of Alberta, Canada. *Journal of Paleontology* **79**, 1189-1213 (2005).

94. Sloan, R. E. Paleontology and geology of the Badwater Creek area, central Wyoming. Part 2. The Badwater multituberculate. *Annals of the Carnegie Museum* **38**, 309-325 (1966).

95. Schumaker, K. K. & Kihm, A. J. Multituberculates from the Medicine Pole Hills local fauna (Chadronian) of Bowman County, North Dakota. *Paludicola* **6**, 9-21 (2006).

96. Jepsen, G. L. Paleocene faunas of the Polecat Bench Formation, Park County, Wyoming. *Proceedings of the American Philosophical Society* **83**, 217-341 (1940).

97. Krause, D. W. Multituberculates from the Clarkforkian Land-Mammal Age, Late Paleocene-Early Eocene, of Western North America. *Journal of Paleontology* **54**, 1163-1183 (1980).

98. Krause, D. W. Multituberculates from the Wasatchian Land-Mammal Age, Early Eocene, of Western North America. *Journal of Paleontology* **56**, 271-294 (1982).

99. Sweetman, S. C. A new species of the plagiaulacoid multituberculate mammal *Eobaatar* from the Early Cretaceous of southern Britain. *Acta Palaeontologica Polonica* **54**, 373-384 (2009).

100. Engelmann, G. F. & Callison, G. in *Vertebrate Paleontology in Utah* (ed D. D. Gillette) (Utah Geological Survey, Miscellaneous Publication 99-1, 1999).

101. Hahn, G. & Hahn, R. Neue Beobachtungen an Plagiaulacoidea (Multituberculata) des Ober-Juras. 2. Zum Bau des Unterkiefers und des Gebisses bei *Meketibolodon* und bei *Guimarotodon*. *Berliner Geowissenschaftliche Abhandlungen* **E28**, 9-37 (1998).

102. Peláez-Campomanes, P., López-Martínez, N., Álvarez-Sierra, M. A. & Daams, R. The earliest mammal of the European Paleocene: The multituberculate *Hainina*. *Journal of Paleontology* **74**, 701-711 (2000).

103. Vianey-Liaud, M. Les Multituberculés Thanetiens de France, et leur rapports avec le Multituberculés Nord-Americains. *Palaeontographica Abt. A* **191**, 85-171 (1986).

104. Kusuhashi, N., Hu, Y., Wang, Y., Setoguchi, T. & Matsuoka, H. New multituberculate mammals from the Lower Cretaceous (Shahai and Fuxin formations), northeastern China. *Journal of Vertebrate Paleontology* **30**, 1501-1514 (2010).

105. Hahn, G. & Hahn, R. Pinheirodontidae n. fam. (Multituberculata) (Mammalia) aus der tiefen Unter-Kreide Portugals. *Palaeontographica Abt. A* **253**, 77-222 (1999).

106. Kielan-Jaworowska, Z. New Upper Cretaceous multituberculate genera from Bayn Dzak, Gobi Desert. *Acta Palaeontologica Polonica* **21**, 35-49 (1970).

107. Smith, T., Guo, D.-Y. & Sun, Y. A new species of *Kryptobaatar* (Multituberculata): The first Late Cretaceous mammal from Inner Mongolia (P. R.

China). *Bulletin - Institut Royal des Sciences Naturelles de Belgique. Sciences de la Terre* **71**, 29-50 (2001).

108. Hahn, G. & Hahn, R. Neue Beobachtungen an Plagiaulacoidea (Multituberculata) des Ober-Juras. 3. Der Bau der Molaren bei den Paulchoffatiidae. *Berliner Geowissenschaftliche Abhandlungen* **E28**, 39-84 (1998).

109. Desui, M. Dental anatomy and ontogeny of *Lambdopsalis bulla* (Mammalia, Multituberculata). *Contributions to Geology, University of Wyoming* **24**, 65-76 (1986).

110. Kusuhashi, N., Hu, Y., Wang, Y., Setoguchi, T. & Matsuoka, H. Two eobaatarid (Multituberculata: Mammalia) genera from the Lower Cretaceous Shahai and Fuxin formations, northeastern China. *2009* **29**, 1264-1288 (2009).

111. Woodward, A. S. On some mammalian teeth of the Wealden of Hastings. *Quarterly Journal of the Geological Society of London* **67**, 278-281 (1911).

112. Lillegraven, J. A. in *Papers in vertebrate paleontology in honor of Morton Green* (eds J. E. Martin & G. E. Ostrander) 46-56 (Dakoterra, South Dakota School of Mines and Technology, Special Paper 3, 1987).

113. Fox, R. C. Cretaceous mammals (*Meniscoessus intermedius*, new species, and *Alphadon* sp.) from the lowermost Oldman Formation, Alberta. *Canadian Journal of Earth Sciences* **13**, 1216-1222 (1976).

114. Eberle, J. J. & Lillegraven, J. A. A new important record of earliest Cenozoic mammalian history: Geologic setting, Multituberculata, and Peradectia. *Rocky Mountain Geology* **33**, 3-47 (1998).

115. Storer, J. E. The mammals of the Gryde Local Fauna, Frenchman Formation (Maastrichtian: Lancian), Saskatchewan. *Journal of Vertebrate Paleontology* **11**, 350-369 (1991).

116. Montellano, M. Mammalian Fauna of the Judith River Formation (Late Cretaceous, Judithian), Northcentral Montana. *University of California Publications in Geological Sciences* **136**, 1-115 (1992).

117. Paleobiology Database. (http://www.paleodb.org).

118. Tong, Y. & Wang, J. A new neoplagiaulacid multituberculate (Mammalia) from the lower Eocene of Wutu Basin, Shandong. *Vertebrata PalAsiatica* **32**, 275-284 (1994).

119. Missiaen, P. & Smith, T. The Gashatan (late Paleocene) mammal fauna from Subeng, Inner Mongolia, China. *Acta Palaeontologica Polonica* **53**, 357-378 (2008).

120. Johnston, P. A. & Fox, R. C. Paleocene and Late Cretaceous mammals from Saskatchewan, Canada. *Palaeontographica Abt. A* **186**, 163-222 (1984).

121. Weil, A. A new species of *Microcosmodon* (Mammalia: Multituberculata) from the Paleocene Tullock Formation of Montana, and an argument for the Microcosmodontinae. *PaleoBios* **18**, 1-15 (1998).

122. Krause, D. W. Paleocene multituberculates (Mammalia) of the Roche Percée local fauna, Ravenscrag Formation, Saskatchewan, Canada. *Palaeontographica Abteilung A* **159**, 1-36 (1977).

123. Scott, C. S. & Krause, D. W. Multituberculates (Mammalia, Allotheria) from the earliest Tiffanian (late Paleocene) Douglass Quarry, eastern Crazy Mountains Basin, Montana. *Contributions from the Museum of Paleontology, University of Michigan* **31**, 211-243 (2006).

124. Wilson, R. W. A new multituberculate from the Paleocene Torrejon fauna of New Mexico. *Transactions of the Kansas Academy of Science* **59**, 76-84 (1956).

125. Hunter, J., Heinrich, R. E. & Weishampel, D. B. Mammals from the St. Mary River Formation (Upper Cretaceous), Montana. *Journal of Vertebrate Paleontology* **30**, 885-898 (2010).

126. Rigby, J. K., Jr. Swain Quarry of the Fort Union Formation, middle Paleocene (Torrejonian), Carbon County, Wyoming. Geologic setting and mammalian fauna. *Evolutionary Monographs* **3**, 1-162 (1980).

127. Wilson, G. P., Dechesne, M. & Anderson, I. R. New latest Cretaceous mammals from northeastern Colorado with biochronologic and biogeographic implications. *Journal of Vertebrate Paleontology* **30**, 499-520 (2010).

128. Matthew, W. D., Granger, W. & Simpson, G. G. Paleocene multituberculates from Mongolia. *American Museum Novitates* **331**, 1-4 (1928).

129. Krause, D. W. Systematic revision of the genus *Prochetodon* (Ptilodontidae, Multituberculata) from the Late Paleocene and Early Eocene of Western North America. *Contributions from the Museum of Paleontology, University of Michigan* **27**, 221-236 (1987).

130. Krause, D. W. *Evolutionary history and paleobiology of Early Cenozoic Multituberculata (Mammalia) with emphasis on the family Ptilodontidae* Ph.D. thesis, University of Michigan, (1982).

131. Scott, C. S., Fox, R. C. & Youzwyshyn, G. P. New earliest Tiffanian (late Paleocene) mammals from Cochrane 2, southwestern Alberta, Canada. *Acta Palaeontologica Polonica* **47**, 691-704 (2002).

132. Gidley, J. W. Notes on the fossil mammalian genus *Ptilodus*, with description of a new species. *Proceedings of the United States National Museum* **36**, 611-626 (1909).

133. Simmons, N. B. A revision of *Taeniolabis* (Mammalia: Multituberculata), with a new species from the Puercan of eastern Montana. *Journal of Paleontology* **61**, 794-808 (1987).

134. Averianov, A. O. & Archibald, J. D. Mammals from the Upper Cretaceous Aitym Formation, Kyzylkum Desert, Uzbekistan. *Cretaceous Research* **24**, 171-191 (2003).